Studies on structural characteristics of aggregated casein clusters and their roles in encapsulation systems

和文題目：カゼイン凝集クラスターの構造的特性とその物質包含系としての役割に関する研究

Teeraya　JARUNGLUMLERT

Contents

Chapter 1

General introduction

The main objective of this work is to study the encapsulation properties and microstructure of the casein cluster prepared from sodium caseinate (SC). SC is water-soluble derivatives of acid milk caseins, produces by reaction with alkali (sodium). Casein and SC have attracted attention in recent decades for use as encapsulants in food and drug delivery systems due to their functional properties (Livney, 2010; Elzoghby et al., 2011). SC can encapsulate materials during forming cluster by simply controlling the pH of the solution. However, the encapsulation behavior and the influence of process conditions on the encapsulation properties of the obtained casein cluster are not fully understood. In this chapter, the concept of encapsulation, the general characteristics of caseins and SC, the encapsulation techniques, and the basic theory of small-angle X-ray scattering, major analytical technique used in this work, are proposed. In the second chapter, the appearance, the microstructure, and the zeta-potential of casein cluster at the different pH values as well as the effect of pH on the encapsulation efficiency (EE) are discussed. The third chapter focuses on the stability and the microstructure of casein cluster when the aging step was applied to the SC solution. Moreover, the re-assembled micelles method was used to prepare casein cluster and their properties were compared with original clusters. In the fourth chapter, digestibility of the obtained casein powder is studied. Additionally, the influence of drying temperature on the properties of casein

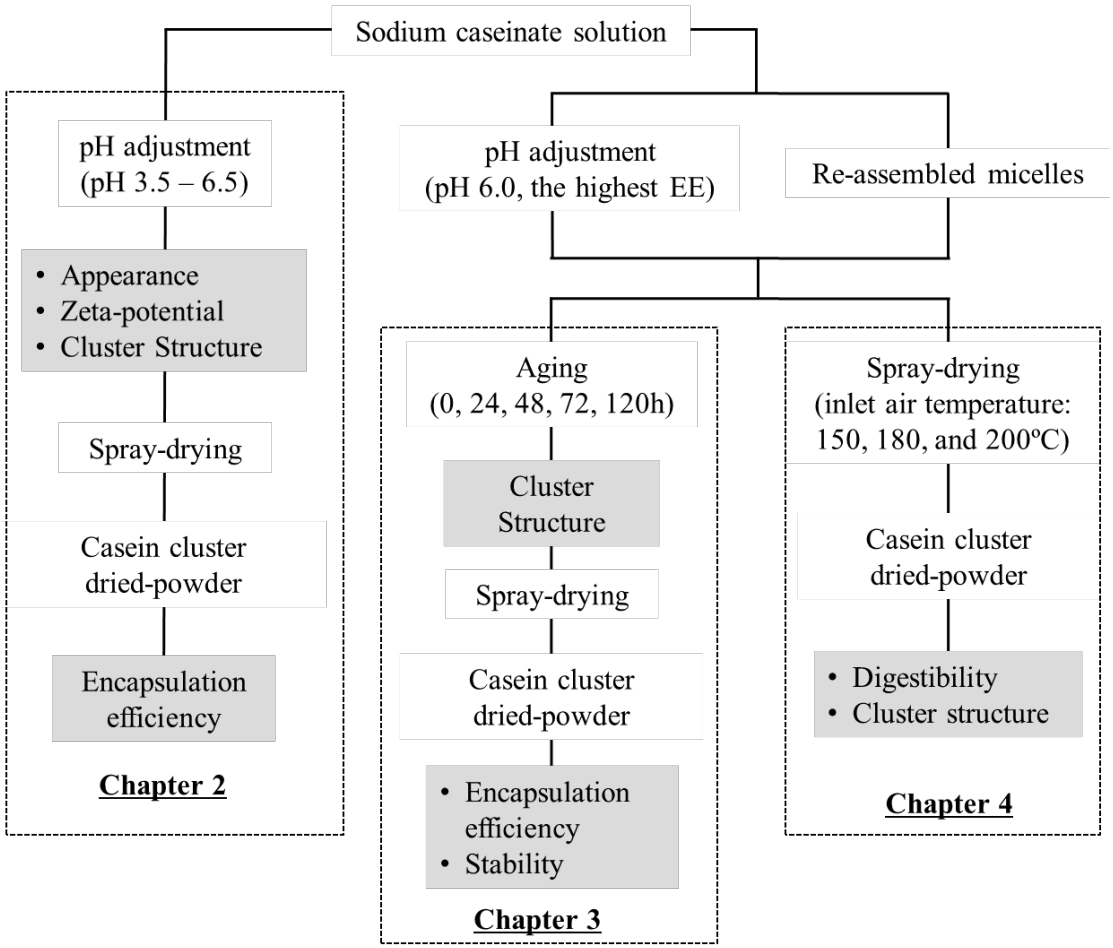

Figure 1–1: The summary diagram of the experimental work and the analysis of sample properties are present in grey boxes.

cluster was also investigated. Summary of the experimental works carried out in this research is schematized in Figure 1–1.

1.1 Encapsulation

Micro- and nano-encapsulation are technique used to entrap one substance within another substance in order to protect them from undesirable degradation. Most of entrapped substances, called the core/encapsulated/entrapped materials, such as drugs, vitamins, vaccine, volatile active agents, microorganisms, etc., are sensitive to

external stress. Encapsulation provides numerous functionalities for example; improving the stability of the core materials by protecting them from their reactivity with the environment, improving the bioavailability and controlled release of entrapped substances, improving the solubility of the hydrophobic compounds, reducing flammability of volatiles, and improving the handling properties of liquid or gaseous materials and keep odors or flavors contained (de Vos et al., 2010; Gonnet et al., 2010; Nedovic et al., 2011; Tavares et al., 2014). The microcapsules have a wide size range of several nanometers to millimeters that can divide into two main types, i.e., the core-shell type and the matrix type (Figure 1–2). For the core-shell type, the core material is surrounding by the shell material (single or multi layers). For the matrix type, the active substance is dispersed in the wall material (Desai & Park, 2005; Zuidam & Shimoni, 2010). Efficient encapsulations are achieved when the maximum possible quantity of core material is encapsulated inside the particles, allowing for high stability, increased shelf-life, and controlled release (Jafari et al., 2008). Large numbers of researches have been reported to study the effects of operating conditions during spray-drying to improve encapsulation efficiency (Liu et al., 2004; Chegini & Ghobadian, 2007).

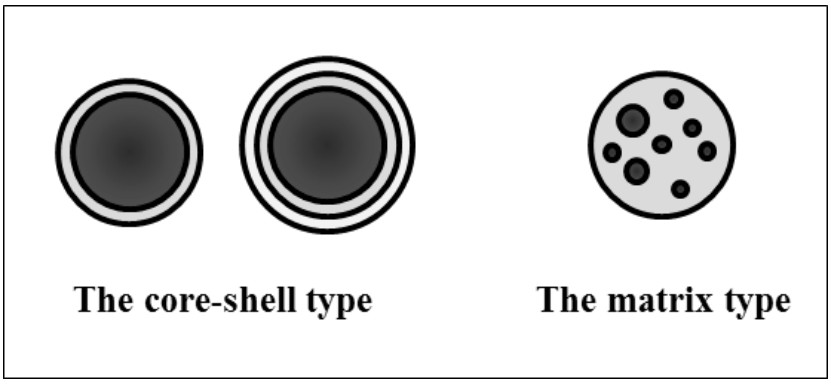

Figure 1–2: Illustration of the encapsulation particles types.

The selection of wall material is of great importance for encapsulation, because the protection or controlled-release features are mainly dependent on the properties of the wall materials employed. Typical substances can be used as wall material; however, biomolecules, e.g., carbohydrates and proteins, are mainly selected for encapsulation, especially in food and pharmaceutical sectors. Due to its advantageous features, carbohydrates are frequently used as wall material for many years (Wandrey et al., 2010). For example, Liu et al. (2005) reported that the gelling characteristic of pectin is effective to increase the bioavailability and the retention time of the dosage form during digestion in drug delivery system. Hydrolyzed starches present good protection against oxidation for orange oil and carrot carotene (Beristain et al., 2002; Wagner & Warthesen, 1995) because of the affinity between their hydrophilic and the hydrophobic compounds (Shaikh et al., 2006). Gum arabic has an excellent emulsification property that produces the stable oil-emulsion over a wide pH range (Gharsallaoui et al., 2007). Krishnan et al. (2005a, 2005b) reported that the stability of food flavors encapsulated in gum arabic was better than maltodextrins and modified starch. Although carbohydrates offer many advantageous properties for encapsulation, most of them are poor in the interfacial properties required for high encapsulation efficiency (Gharsallaoui et al., 2007).

Proteins have superior interfacial properties over carbohydrates, and thus they have been largely used as wall material for hydrophobic bioactive compounds (Tavares et al., 2014). Many researchers reported that proteins and flavors compounds were linked together by hydrophobic and hydrogen bonding and the binding strength is directly affecting their release property (Fares et al., 1998; Guichard, 2006; Landy

et al., 1995). The controlled release property of proteins has been growing interest to study and develop drug delivery system. Controlled release of drug means controlling drug dosage and reducing the effect of excess intake of drug (Elzoghby et al., 2012; Tavares et al., 2014). Proteins have been reported as a successful in delivery and controlled release of various drugs, for example the encapsulation of tizanidine hydrochloride, gatifloxacin and fluconazole in gelatin (Lee et al., 2012), the dermal drug encapsulated with collagen nanoparticles (Lee et al., 2001), and anticancer drug loaded with casein (Elzoghby et al., 2013a; Shapira et al., 2010a).

Quality of the encapsulation products depends not only on the characteristic of wall or core materials but also on the preparation technique. Numerous techniques have been developed for encapsulation and each technique is applicable to some wall and core materials, so the selection of encapsulation technique must carefully be considered. Basic steps, suitable wall and core materials, advantages, and weakness of commonly used encapsulation techniques are summarized in Table 1–1.

Table 1–1 Overview of commonly techniques used for the encapsulation active ingredients (Beristain et al., 1996; Black et al., 2014; Desai & Park, 2005; Gibbs et al., 1999; Okuro et al., 2013; Sanchez et al., 2013; Tavares et al., 2014; Zuidam & Shimoni, 2010)

Technique	Basic steps	Core materials	Wall materials
Spray-drying	- Preparation of the dispersion or emulsion of core materials in the wall materials. - Atomization and dehydration of the dispersion or emulsion.	Food ingredients, drug, flavor, hydrophobic substances, vitamins, fatty acid, etc.	Carbohydrates such as gum acacia, maltodextrins, modified starch, polysaccharides etc. Proteins such as whey proteins, soy proteins, sodium caseinate, etc.
	Advantage: Low operation cost, flexible, and produces good quality of encapsulation products. **Disadvantage**: Wall material used for spray-drying must have a good solubility in water and high temperature is used in the process.		
Spray-cooling/ chilling	- Preparation of the dispersion or emulsion of core materials in the wall materials (often vegetable oils). - Atomization and cooling of the dispersion or emulsion, then micro-capsules are formed (no mass transfer).	Frozen liquids, heat-sensitive materials, water-soluble substances such as minerals, water-soluble vitamins, enzymes, flavors, fragrances and probiotics.	Typically some form of vegetable oil (in the case of spray-cooling, 45 to 122°C) or its derivatives (in the case of spray-chilling, 32 to 42°C) as well as fat, stearin, mono- and di-acylglycerols.
	Advantage: Low operation cost, simple to apply and scale up and no organic solvents used. **Disadvantage**: Limitation of wall materials, require special handling and storage conditions.		

Technique	Basic steps	Core materials	Wall materials
Extrusion	- Preparation of core materials. - Core materials are immersed in a hardening bath with wall materials, micro-particles are formed.	Mainly used for food flavors, vitamins and colors.	Carbohydrates such as sucrose, maltodextrin, glucose syrup, etc.
	Advantage: Produces high stability encapsulation particles because the core materials are completely surrounded by wall materials. **Disadvantage**: Low encapsulation efficiency.		
Fluidized bed	- Preparation of wall materials. - Wall material is atomized onto core material fluidized by top-spray, bottom-spray, or tangential-spray.	Usually use for isolate iron from ascorbic acid in multivitamins, encapsulate heat sensible substances such as vitamins and minerals.	Carbohydrates and hot-melts materials for example vegetable oil, waxes and fatty acids.
	Advantage: Wide variety of wall materials can be use. **Disadvantage**: Core materials must be solids and have a narrow size distribution.		
Lyophilization/ freeze-drying	- Prepare the mixture of core and wall materials. - The mixture is rehydrated by freeze-drying.	Heat sensitive and high value substances such as drugs, probiotics, and aromas.	Carbohydrates and proteins.
	Advantage: Suitable for thermal-sensitive substances. **Disadvantage**: Extremely high operation cost and the obtained encapsulation particles are non-uniform.		
	Advantage: Uncomplicated process and no elaborate manufacturing equipment are requiring. **Disadvantage**: High operating cost and cross-linking of the wall material usually involves harmful chemicals, e.g. glutaraldehyde.		

Technique	Basic steps	Core materials	Wall materials
Cocrytallization	- Preparation of the supersaturated wall material solution (sucrose). - Addition of core materials. - Forming a crystalline irregular network to encapsulate core materials.	Acids, flavors, antioxidants, and minerals.	Sucrose
	Advantage: Dried particles can be obtained without additional drying process and high encapsulation efficiency.		
	Disadvantage: Wall material must be crystallized.		

1.2 Caseins and caseinates

Caseins are major protein components found in milk (approximately 80% of total milk protein). They consist of four main protein fractions, α_{s1}-, α_{s2}-, β-, and κ-caseins, which offer high nutritional value since they contain approximately 94% proteins and 6% minerals, i.e. calcium, phosphate, magnesium, citrate and all essential amino acids required for bone growth (Fox & McSweeney, 2003; Fox & Brodkorp 2008). Caseins exhibit excellent interfacial properties, thermal stability, and biodegradability, and they are classified as generally recognized as safe (GRAS) (Livney, 2010; Elzoghby et al., 2011). They have been commonly used as an ingredient in foods to improve their physicochemical properties over the last several decades, for example used as emulsifiers in cheese products, used as stabilizer and improve texture of ice-cream, and used to improve nutritional value of pasta and snack. Commercial caseins are prepared from skim milk by acid precipitation or rennet coagulation. Most of caseins (*ca*. 80%–95%) in normal milk form as micelles. These casein micelles are spherical in shape and they are extremely stable with good solubility, good surface activity, and heat resistant that only temperature more than 120°C causes the casein aggregation gradually occur. The general characteristics of casein micelles are summarized in Table 1–2. Commercial acid and rennet caseins are insoluble in water, therefore caseinates are produced. Caseinates are produced by re-solubilized acid/rennet caseins under alkaline conditions (sodium or calcium) and dried to obtain caseinates powder. They exhibit superior water solubility and thermal stability compared to other proteins (Anarjan et al., 2011). Sodium caseinate can aggregate into large particles by reducing pH of the solution. The aggregation number

slightly increases with reducing pH from 8 to 6, but extremely increases at lower pH values (HadjSadok et al., 2008).

Table 1–2 The general characteristics of casein micelles (Fox & Brodkorp 2008).

Characteristic	**Value**
Diameter	range from 50 to 600 nm (mean ≈ 150 nm)
Molecular weight	10^6–10^9 Da (mean ≈ 10^8 Da)
Surface area	8×10^{-10} cm^2
Volume	2.1×10^{-15} cm^3
Density (hydrate)	1.0632 g/cm^3
Mass	2.2×10^{-15} g
Water content	63%
Hydration	3.7 g H_2O / g protein

It is well known that the functional properties of casein depend on their structure and surface properties. Caseins are proline-rich protein including both hydrophilic and hydrophobic domains (Fox & McSweeney, 2003). Numerous studies have been conducted to investigate the unique structure of casein and are presented in various models. Main accepted models and be used as basis of the further model are the coat-core model and the sub-units model. The concept of the coat-core model is the protein at the core of micelle is different from those on the surface (McMahon & McManus, 1998). Model proposed by Waugh and Noble (1965) and Waugh et al. (1970) is relate to the coat-core model that the layer of κ-caseins surrounding the α_s- and β-caseins core. The size of micelle was controlled by the amount of the κ-caseins available and its stability depended on the amount of calcium. For the sub-units model, casein aggregates are formed by the hydrophobic interaction of many roughly spherical sub-units (or sub-micelles) that are about 12–15 nm in diameter, the model

image of casein micelles supposed by Walstra (1999) can be seen in Figure 1–3. Two main types of sub-units, κ-caseins rich and poor, are held together by the formation of intermolecular disulfide bonds of the κ-caseins rich sub-units (Dalgleish & Corredig, 2012). The κ-caseins rich sub-units are present mainly at the edge of micelles with the hydrophilic end of the protruding peptide chain that appear to be "hairy" layer. This layer will obstruct the further aggregation of sub-units and by steric and electrostatic repulsion, in the other word, micelles stability is related to the hairy layer of κ-caseins (Walstra, 1999).

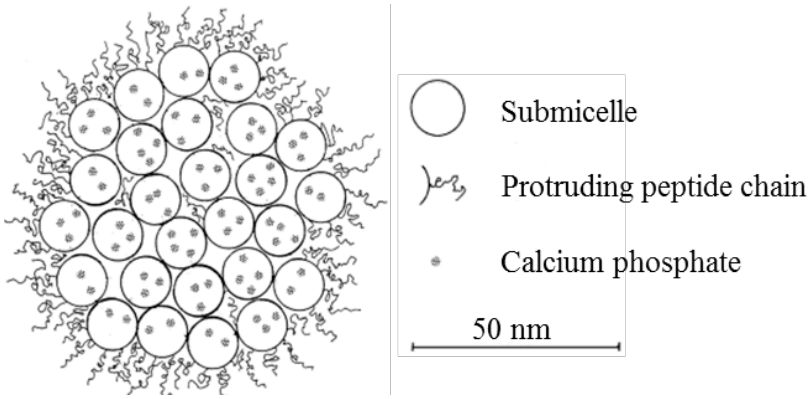

Figure 1–3: The casein micelles image of sub-units model supposed by Walstra (1999).

1.3 Caseins and caseinates used as natural vehicles

Due to the unique physicochemical properties and functionalities of casein and their products make them highly suitable to use as vehicles for delivering various active substances. Important step that directly affects to the quality, properties, and stability of final product is the formation of caseins particles or how they link with the

encapsulated substances. A number of strategies have been developed and used to prepare the caseins encapsulation products.

1.3.1 Self-assembly and co-assembly

Self-assembly feature of casein can be employed to encapsulate various active substances. Caseins are organized in nano- or microstructure mainly by hydrophobic and electrostatic interactions and they can incorporate with active substances upon the formation. Numbers of researchers studied in the self-assembly and co-assembly casein-based encapsulation applied with many different systems. Purified β-casein micelles extracted from fresh milk were co-assembled with curcumin by simply mixed them in ethanol, subsequently evaporation of solvent. The solubility and the cytotoxicity of curcumin were successfully improved by this system (Esmaili et al., 2011). Similarly as the method of Pan et al. (2013), they dissolved sodium caseinate and cucumin in a warm aqueous ethanol to improve the solubility of curcumin. They proposed the formation mechanism of casein, as shown in Figure 1–4, that sodium caseinate dissociated to small structures in a warm aqueous ethanol, and then re-formed into nanoclusters after spray-drying and rehydration. Curcumin was entrapped in casein nanoclusters during their reformation via hydrophobic interactions confirmed by fluorescence spectroscopy. Dissociation followed by re-assembly micelles of casein has also been reported by Menéndez-Aguirre et al. (2011). The dissociation of casein was induced by high pressure treatment with and without calcium and phosphate ions. The results demonstrated that loading amount of vitamin D_2 on the re-assembled casein could be enhanced by this process. Semo et al. (2007) reproduce casein micelles from sodium caseinate by setting up condition similar to the

original milk. This re-assembled micelle was used as encapsulating agent for vitamin D_2. Shapira et al. (2010a, 2010b) proposed model to explain the co-assembly mechanism between β-casein and hydrophobic drugs that drug would priory associate with β-casein by hydrophobic interactions, and subsequently with electrostatic affinity. This model is similar as the model proposed by Martinez et al. (2011) that explained about a self-assembly behaviour of the casein glycomacropeptide.

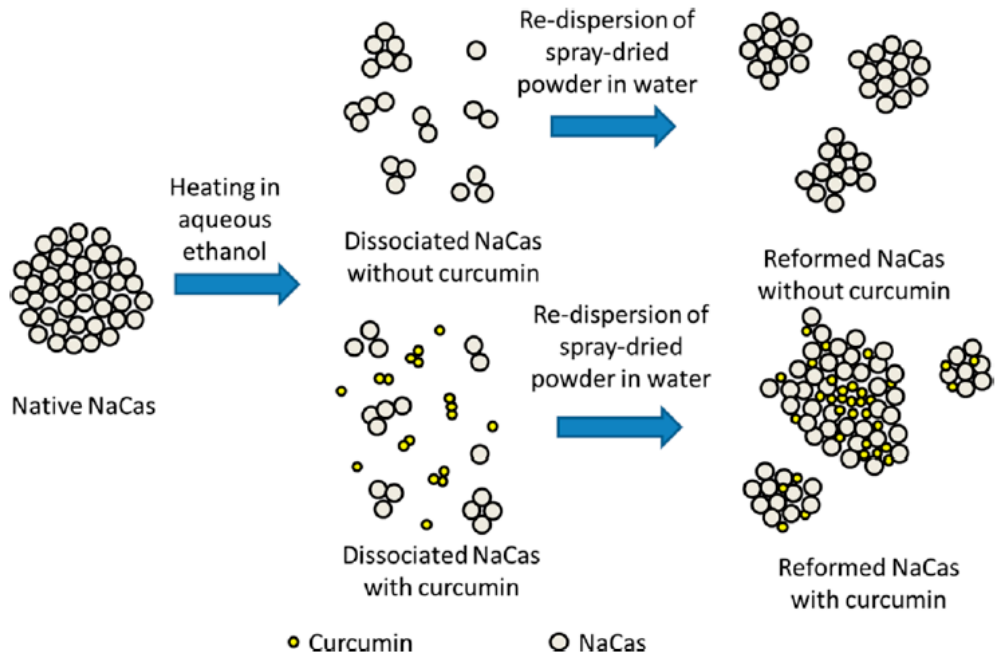

Figure 1–4: The formation model of sodium caseinate incorporation with curcumin proposed by Pan et al. (2013).

1.3.2 Emulsification

Due to the excellent interfacial properties of caseins products, especially sodium caseinate, they would appear to offer the suitable properties required to encapsulate lipid substances. Lim et al. (2012) reported that sodium caseinate was the

most effective wall material for encapsulate pitaya seed oil by emulsification that it gave the highest in oil retention compared with whey protein and gum arabic. Chung et al. (2010) attempted to improve the EE of sodium caseinate microcapsules by combining with resistant starch (RS) for encapsulate fish oil. The RS used in this work was modified by heating (Heat RS) or followed by microfluidization (Heat-MF RS). Combination of caseinate and Heat-MF RS succeeded to improve the EE, whereas it was poor to protect the encapsulated oil from oxidation. Numerous other researchers interested in the influences of the processing condition during emulsification on the characteristics of casein encapsulation products, for example effects of the homogenizer pressure on the emulsion morphology (Anarjan et al., 2011; Hogan et al., 2001; Qian & McClements, 2011) and effects of the sodium caseinate concentration on the stability and emulsion microstructures (Tan & McGrath, 2012).

1.3.3 Chemical crosslinking

Crosslinking is the process to connect two or more molecules together with chemical links (Jyothi et al., 2010). Elzoghby et al. (2013a, 2013b) succeeded to use a genipin as a crosslinker to improve the stability of casein-drug nanoparticles. A genipin in ethanol was simple added into the casein-drug mixture, subsequently spray-drying. Color of the mixture turned from transparent to dark blue derived from the double bonds of the genipin crosslinked molecules. This research group also applied the crosslinked casein with the polyanionic crosslinker sodium tripolyphosphate to encapsulate an anticancer drug flutamide. The half-life of this

drug greatly increased and their biodegradability was depending on the density of crosslinked molecules (Elzoghby et al. , 2013c).

1.4 Small and ultra-small angle X-ray scattering technique

Small angle X-ray scattering (SAXS) and ultra-small angle X-ray scattering (USAXS) is a powerful technique for investigating the structure of macromolecules in solution without the limitation of molecular weight, such as proteins, nucleic acids, polymers, colloid, as well as metal aggregates. SAXS and USAXS can observe the particles in the size range of 1–100 nm and 100–10,000 nm, respectively. To understanding the structural characteristics of large aggregates, the combination of SAXS and USAXS can be used to evaluate the structures of macromolecules since it provides information about clusters ranging from one to several thousand nanometers (Zhang and Ilavsky, 2010). Particles in the sample solution will scatter their signal out, when they are attacked by X-rays beam. The generated 2D scattering pattern from the macromolecules is generally converted to one dimension profiles (Koch et al., 2003; Mertens & Svergun, 2010). The schematic of the basic SAXS experiment is shown in Figure 1–5. From the scattering profile, important parameters can be obtained and used for analysed the structural characteristics of sample. Numerous studies on the higher order structures of bio-macromolecules have been carried out by using SAXS measurement. Moitzi et al. (2008) evaluated the effects of temperature and pH on the shape, structure, and aggregation number of β-casein micelles using SAXS measurements. The results suggested that the shape and dimensions of the micelles varied depending on the preparation conditions. SAXS has also been applied to the investigation of the effects of environmental factors on the sub-structure of casein

micelles (Marchin et al., 2007). Pignon et al. (2004) analyzed casein micelles with SAXS and USAXS, and the results showed that casein micelles are bimodally distributed with two size length scales of around 100 nm for the globular micelles and 5.6 nm for the sub-micelles.

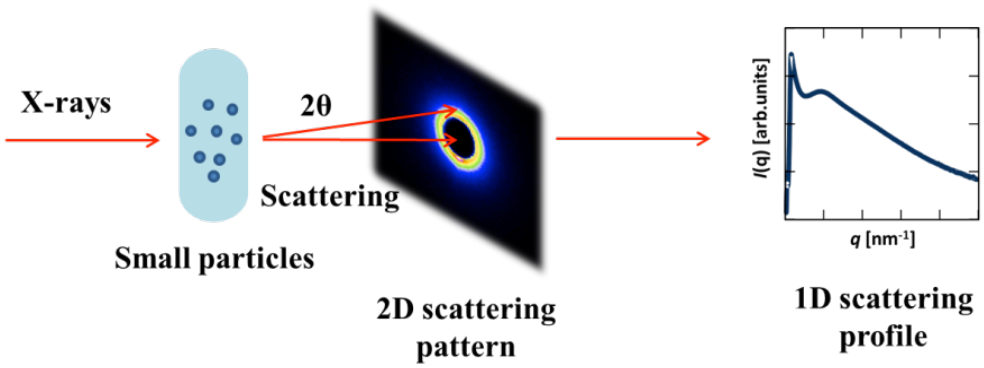

Figure 1–5: The schematic of the basic SAXS experiment.

1.4.1 SAXS analysis

The obtained 2D scattering patterns were integrated to obtain the 1D profiles, and the scattering intensities, I(q), were plotted against the q values after subtraction of the background intensity (scattering intensity of the capillary filled with the blank solution). The q is magnitude of the scattering vector, (q=(4π/λ)sinθ, where 2θ is the scattering angle). The obtained scattering profiles were used to calculate the structural parameters, i.e., radius of gyration (R_G), zero intensity (I(0)), and fractal dimensions (D), using the following scattering model equation (Freltoft, 1986; Sorensen, 1992):

$$I(q) = \frac{\sin[(D-1)\arctan(q\xi)]}{(D-1)q\xi(1+q^2\xi^2)^{(D-1)/2}} \qquad (1\text{–}1)$$

This equation is based on the exponential cutoff for fractal objects, $h(r/\xi) = e^{-r/\xi}$, where $\xi^2 = 2R_G^2/(D(D+1))$. The present casein clusters were assumed to exhibit fractal morphology, since they are composed of many primary casein particles. In order to consider the cluster density, the $I(0)/R_G^3$ value was used as an indicator, termed the density index (δ), where R_G is related to cluster size and $I(0)$ corresponds to the molecular weight of the scattering cluster.

The SAXS and USAXS profiles were combined to investigate the structures of materials in the nano- to micro-meter scale. The analyses were carried out in two regions corresponding to the two structural size scales: (i) low q range (0.004–0.06 nm^{-1}, which correlates to dimensions of approximately 100–1600 nm in real space), where the intensity obtained from USAXS measurements reflects the characteristics of the whole cluster domains; and (ii) high q range (0.06–2.0 nm^{-1}, which correlates to dimensions of approximately 3–100 nm in real space), where the intensity obtained from SAXS measurements is scattered from smaller domains, mainly reflecting the primary cluster (Figure 1–6). The D value is an absolute value of the power law exponent of the scattering profile, $I = q^{-(D^L or D^H)}$, where D^L is determined from the lower q region and D^H is determined from the higher q region. The value of D is used to distinguish the characteristics of fractal objects; surface fractals ($3 \leq D \leq 4$) relate to particles with rough or smooth surfaces, and mass fractals ($1 \leq D < 3$) relate to particles with branched and crosslinked network structures.

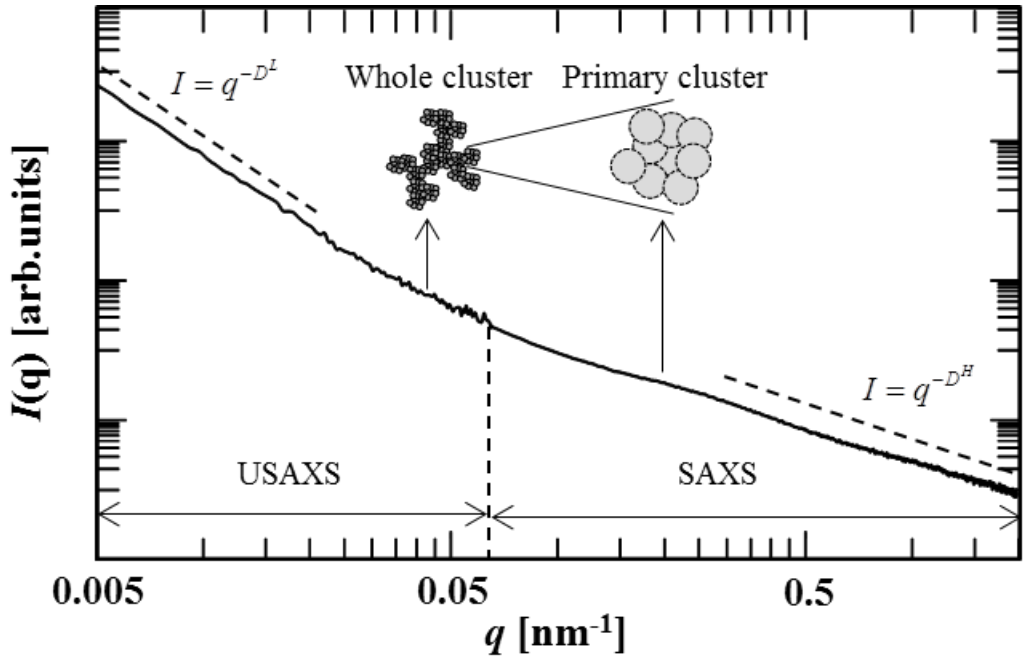

Figure 1–6: Combination of ultra-small-angle X-ray scattering (USAXS) and small-angle X-ray scattering (SAXS) profiles and an illustration of a cluster corresponding to the *q* region.

Chapter 2

Influences of acidic conditions on the properties and encapsulation efficiency of the casein cluster loaded β-carotene

2.1 Introduction

Casein and caseinate have been shown to form clusters through hydrophobic interactions by simply controlling the pH of the prepared solution. Prior studies have shown that pH, temperature, and ionic strength are critical factors that determine the formation of casein micelles/clusters. Furthermore, the kinetics of cluster formation is closely linked to the properties of encapsulant (Anema et al., 2004; Guillaume et al., 2004; Jaubert et al., 1999; McSweeney et al., 2004). HadjSadok et al. (2008) reported that the decreasing pH of caseinate solution between pH 8.0 and 6.0 resulted in small increase of the aggregation number, whereas extensive aggregation occurred when the pH was lower than 6.0. Ruis et al. (2007) also reported in the same way that the stickiness of the caseinate aggregates was dependent on the pH of the solution. Previous studies have shown that the aggregation of caseinate induced by pH changes can entrap hydrophobic substances in the cluster; e.g., curcumin (Pan et al., 2013, 2014) and bixin (Zhang & Zhong, 2013). Although various aspects of the formation mechanisms of casein micelles/clusters have been studied, investigations that correlate cluster formation kinetics to the properties of the resultant dried products are still lacking. This chapter aims to investigate the effects of pH values on the EE and aggregation behaviours of SC. We used β-carotene as a core material model and

determined the EE of the prepared spray-dried cluster by the measured release rate of β-carotene. The surface characteristics of the aggregated casein clusters were analyzed by small angle X-ray scattering (SAXS), cluster size, and zeta (ζ)-potential measurements.

2.2 Materials and methods

2.2.1 Materials

Sodium caseinate (SC) from bovine milk and β-carotene (type I, synthetic, ≥93%) were purchased from Sigma-Aldrich (St Louis, MO, USA). Acetic acid was purchased from Wako Pure Chemical Industries, Osaka, Japan. All chemicals used were of analytical grade.

2.2.2 Particle preparation

SC was dissolved in distilled water at a concentration of 5.0% (w/v). After stirring for 2 h, the SC solution was mixed with 2 mL of β-carotene solution (β-carotene dissolved in acetone with β-carotene:SC ratio of 1:200); the resultant mixture was stirred overnight. The pH values of the solutions were adjusted to desired values by adding acetic acid and were monitored by a pH meter (SK-620PH, Sato Keiryoki Mfg Co., Tokyo, Japan). The prepared solution was spray-dried with a laboratory-scale mini spray dryer B-290 (Büchi Labortechnik AG, Switzerland) equipped with a 0.7 mm diameter nozzle. The operational conditions of spray-drying were as follows: inlet drying air temperature, 110°C; outlet temperature, 80°C; pump rate, 145 mL/h; aspirator rate, 90%; and spray-drying air flow rate, 350 mL/h. The obtained dried powders were kept in tightly capped vials and stored in dark until

analysis. The specimen IDs of the prepared spray-dried powders are listed in Table 2–1 with the specifications.

Table 2–1 Specification of the specimens.

Specimen ID	pH	note
A70	-	Without any pH adjustment
A65	6.5	
A60	6.0	
A55	5.5	

2.2.3 Encapsulation efficiency (EE) measurement

The β-carotenes in the dried specimen were extracted into an ethanol solution as follows: 0.1 g of the specimen was put into 4 mL of ethanol, shaken for 15 s, and then stored in dark for the desired time. After centrifuging the solution for 1 min, the supernatant was collected and the absorption intensity was measured at 450 nm using an ultraviolet-visible (UV-vis) spectrophotometer (Nanodrop2000C, Thermo Fisher Scientific Inc., USA). The quantities of β-carotene extracted in the initial 15 s were used to estimate the amount of free β-carotene. The quantities obtained after extraction over 24 h were used to evaluate the total β-carotene loaded. The EE was calculated with the following equations:

$$\text{Free } \beta\text{-carotene} = \left[\frac{\text{Extracted amount of } \beta\text{-carotene after 15 s}}{\text{Total } \beta\text{-carotene load in the original solution}} \right] \times 100 \qquad (2\text{–}1)$$

$$\text{Encapsulation efficiency (EE)} = \left[\frac{\text{Extracted amount of } \beta\text{-carotene after 24 h} - \text{Free } \beta\text{-carotene}}{\text{Total } \beta\text{-carotene load in the original solution}} \right] \times 100 \qquad (2\text{–}2)$$

The total mass of β-carotene loaded in the original solution was used to standardize the EE.

2.2.4 Particle size and ζ-potential measurement

Particle size and ζ-potential of the casein cluster in distilled water were determined using dynamic light scattering, DLS, (Zetasizer NanoZS, Malvern Instruments, Worcestershire, UK). SC was dissolved in distilled water at concentrations of 0.5%, 1.0%, and 5.0% (w/v). After 2 h of stirring, the pH of the casein suspension was adjusted to the desired value by adding aqueous acetic acid solution.

2.2.5 Characterization of casein clusters by SAXS

SAXS measurements were performed at the beamline BL40B2 at Spring-8 (Hyogo, Japan). The wavelength (λ) of the beam was 0.1 nm. A 30 cm^2 imaging plate was used to record the scatter profiles, with the detector placed 4,166 mm away from the sample, providing a q range of 0.05–2.0 nm^{-1}. The test solution was filled in a sample holder (1 mm thickness) and placed on the sample stage. The SAXS data were recorded with an exposure time of 10 s.

2.3 Results and discussion

2.3.1 ζ-Potential

ζ-Potential is present between the particle surface and dispersing liquid. Its magnitude indicates the stability of the colloidal system. The ζ-potentials of a 0.5% (w/v), 1.0% (w/v), and 5.0% (w/v) SC solution at different pH values are shown in Figure 2–1(A). SC solutions possessing a pH value between 7.0 and 5.0 were found to be negatively charge and displayed no net charge at approximately pH 4.4, indicating their isoelectric point. The magnitude of the ζ-potential increased as the pH

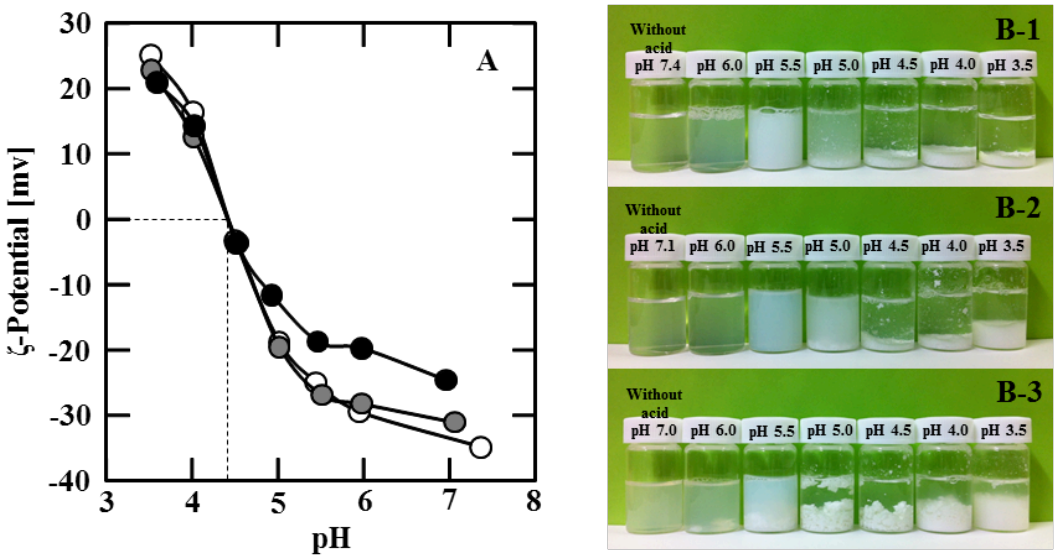

Figure 2–1: (A) Zeta (ζ)-potential for SC solution: 0.5% w/v [○], 1.0% w/v [◍], and 5.0% w/v [●]; and (B) appearance of SC solution as a function of pH; (B-1) 0.5% w/v, (B-2) 1.0% w/v, and (B-3) 5.0% w/v.

values decreased. The appearance of the prepared solutions corresponded well with the observed ζ-potential values (Figure 2–1(B)); though the SC solutions were transparent, they became turbid at pH lower than 5.5, indicating the formation of

aggregated casein particles. When the pH values became lower than the isoelectric point, the aggregated clusters in the solution began to precipitate.

2.3.2 Encapsulation efficiencies

The central motivation of this work was to study the influence of pH values on the resultant encapsulation properties of spray-dried casein clusters; accordingly, we measured the release rate and EE of the encapsulated β-carotene in ethanol in order to assess these properties. SC at a concentration of 5.0% (w/v) was used to encapsulate β-carotene (β-carotene:SC = 1:200). The EE were higher at lower pH values (pH 6.0–7.0), with values varying from 20% to 29% and the free β-carotene was approximately 1–7% (Figure 2–2). When the specimen was prepared from a solution with pH 6.0, the EE was maximized. These results suggest the importance of the kinetics of the structural modifications of particles on the encapsulation properties of the resultant dried powders. The release curves of β-carotene from the dried specimen are shown in Figure 2–3. Approximately 50% of the encapsulated β-carotene was released within the first 1 h; the release rates for the specimens tested were similar to each other. Further, after 6 h, 83%, 81%, 70%, and 69% of the encapsulated β-carotene was released from the dried particles A55, A70, A60, and A65, respectively. The A55 had the highest surface β-carotene loading (approximately 7%), whereas those of the other specimens (A70, A65, and A60) were found to be in the 1–3% range. This suggests that the rapid aggregation under highly acidic conditions provided ideal conditions for the entrapment of β-carotene in the aggregated particles; however, many β-carotenes were found at the surface.

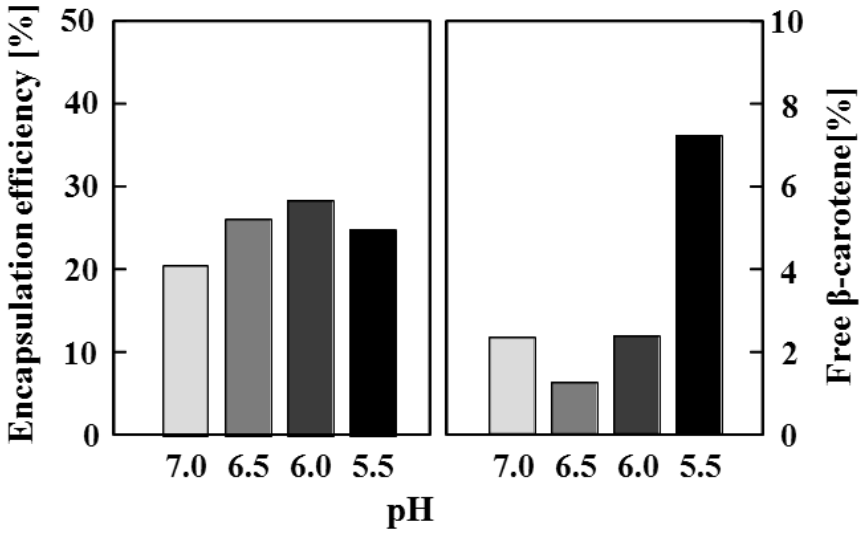

Figure 2–2: Encapsulation loading efficiencies with respect to pH of solution.

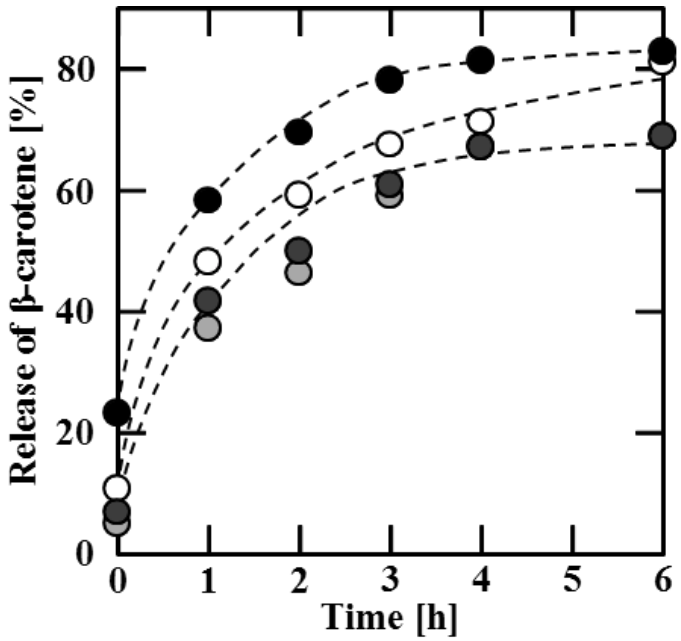

Figure 2–3: The release of β-carotene from dried casein cluster prepared SC solution: without pH adjustment [○], pH 6.5 [◔], pH 6.0 [◕], and pH 5.5 [●].

2.3.3 Size and surface characteristics

SAXS measurements were carried out to determine how the formation of aggregated casein clusters and surface characteristics were affected by pH values to provide support for the results described in the previous section. Figure 2–4 shows the scattering profiles of the SC solutions obtained from four different pH values, A70, A65, A60, and A55, where scattering intensity, I(q), was plotted against q in the range $0.001 < q < 0.12$. It was found that the scattering intensities obtained from solutions of A55 were clearly higher than those of the others, especially in the lower q region, an outcome thought to be due to the aggregate formation. The discrepancies in these profiles indicated that the structures of these specimens were significantly different on the measured scale.

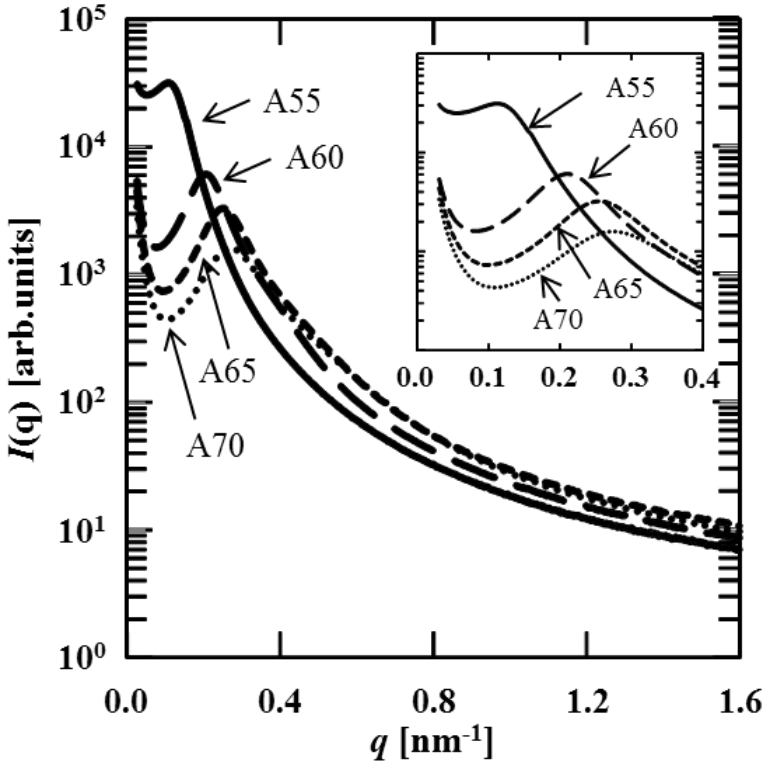

Figure 2–4: Small angle X-ray scattering profiles.

The scattering profile also reflected the fractal structure of the scattering medium. The fractal dimensions in this chapter were simply calculated from the slope of the logarithmic plot between I(q) and q, D = n (i.e., $I(q) \sim q^{-n}$). The scattering profiles were analyzed in the q range of 0.4–0.9. The obtained D values and the mean particle sizes analyzed by DLS measurement are listed in Table 2–2. The D values of the A65, A60, and A55 were approximately 3.6, 3.2, and 3.1, respectively. As explained in 1.4.1, if the D value lay in the range of 3–4, this D value would reflect the characteristic at the surface of cluster, D value close to 4 indicate the smooth surface. Considering with the mean particle sizes, D values corresponded to the increase of the particle sizes when the pH of the SC solution was down from 6.5 to 5.5. So, this aggregate growth was a fractal growth, that is, a random fractal structure formed in the aggregated particle. We opine that this fractal growth nature influenced the encapsulation efficiencies. As discussed in the earlier sections, A60 was found to have the highest encapsulation efficiency. The encapsulation tests suggested a difference in the structures among the different aggregated specimens. The SAXS data clarified that the present aggregations represented a fractal growth system, wherein the randomness of the surface increased with increasing cluster size. It was noteworthy that A60 was the best among the tested specimens, which suggested that there existed an optimal aggregation degree, which maximized the performance of an encapsulated system. Consequently, it is important to control the aggregation kinetics during the syntheses of aggregation-based encapsulation systems.

Table 2–2 Mean particle sizes and fractal dimension of the specimens

Specimen ID	Mean particles sizes [nm]	*D*
A70	155.9	3.6
A65	175.7	3.6
A60	221.2	3.2
A55	289.5	3.1

2.4 Conclusions

In this chapter, the influences of pH on the encapsulation properties and the aggregated structure of casein cluster were studied. We found that the pH of the sodium caseinate solution, which determined the degree of the aggregation, immensely affected the encapsulation efficiencies of β-carotene in the spray-dried powder. Among the examined pH conditions (pH = 6.5, 6.0, and 5.5), pH 6.0 yielded excellent encapsulation efficiency and storage stability. The size of the clusters increased with decreasing pH in the following order: 5.5 < 6.0 < 6.5. Also, the surface fractal dimension increased in the same order. Thus, these differences were linked to the encapsulation characteristics, and suggested that there would be an optimal aggregation degree, which maximized the performance of the encapsulated systems.

Chapter 3

Influences of cluster formation and aging on the encapsulation efficiency and stability of the casein cluster loaded β-carotene

3.1 Introduction

Due to the results of preliminary study in the second chapter that the aggregation of casein induced by pH changes is an important factor that impacts the EE. We found that reducing the pH from neutral to 6.0 effectively enhanced the amount of entrapped β-carotene; however, further reducing the pH from 6.0 to 5.5 decreased the loading amount of β-carotene. The cluster structure obtained from the different pH condition also different. These suggested the importance of clarifying the details of the structural change and kinetics of casein clusters in solution. However, several researchers have suggested that the casein micelle re-assembled from caseinate solution was also effective to encapsulate hydrophobic substances (Sáiz-Abajo et al., 2013; Semo et al., 2007; Zimet et al., 2011). These re-assembled casein micelles were used to encapsulate and deliver hydrophobic substances such as β-carotene, vitamin D_2, and omega-3 polyunsaturated fatty acids. The results suggested that the casein micellar form protected the entrapped substances against environmentally induced degradation and oxidation. Knoop et al., (1979) studied the synthesis of casein micelles by various techniques. Their studies showed that the sub-structure of the synthesized casein micelles prepared by adding calcium,

phosphate, and citrate ions to the caseinate solution was the same as that of natural casein.

In this chapter, the casein cluster obtained by adjustment of pH to ca.6.0 was selected to compare the encapsulation properties with the clusters prepared by re-assembly micelle system. Moreover, the influence of aging sample solution before drying on the EE, the cluster structure, and storage stability was also investigated.

3.2 Materials and methods

3.2.1 Materials

Tri-sodium citrate, di-potassium hydrogen phosphate, calcium chloride, lithium chloride, sodium chloride, sodium azide, hexane, and acetone were purchased from Wako Pure Chemical Industries, Osaka, Japan. All other chemicals were the same as described in 2.2.1.

3.2.2 Particle preparation

The preparation method used in this chapter was modified from the method in the 2nd chapter. Due to the type of spray dryer used, pilot scale with an atomizer, volume of the specimen solution and drying condition were adjusted. A 5.0% (w/v) solution of SC was prepared by dissolving SC in distilled water under overnight stirring at ambient temperature to ensure complete dissolution. β-Carotene in acetone was added to the SC solution, where the mass ratio of β-carotene to SC was 1:400. The mixture was stirred in a thermostatic bath at 37°C for 2 h. Aggregated casein clusters were obtained by gradually reducing the pH (to *ca*. 6.0) using acetic acid

solution, and the pH was measured with the help of a pH meter. The freshly prepared solution was stored for aging under ambient conditions for a selected duration (0, 48, 72, and 120 h). Sodium azide (0.05 g) was added to 500 mL of the final solution to prevent microbial growth during storage. The dried powders were then obtained by spray-drying the prepared solution using an LB-8 spray dryer with an atomizer (Ohkawara Kakohki Co., Yokohama, Japan). The operational conditions were as follows: inlet air temperature: 150°C, outlet air temperature: 110°C, rotational speed of atomizer: 5,000 rpm, and feed flow rate: 10 mL/min. The specimen obtained from this method was named A60 and the specimen prepared without pH adjustment was named A70.

Aggregated casein micelles were prepared by using the re-assembly method reported by Semo et al. (2007). A solution of SC was prepared by dissolving 25 g of SC powder in 400 mL distilled water. After continuous overnight stirring, β-carotene in acetone was added to the solution containing completely dissolved SC, in which the mass ratio of β-carotene to SC was 1:400. A 10 mL aliquot of 1 mol/L tri-sodium citrate was added to the mixture of SC solution and β-carotene. Subsequently, 30 mL of 0.2 mol/L K_2HPO_4 and 36 mL of 0.2 mol/L $CaCl_2$ were added to the prepared solution. These compounds were added in 12 portions over 10 minute intervals under continuous stirring in a thermostatic bath at 37°C. The pH of the final solution was adjusted to 6.7 using 1% of acetic acid solution. The prepared solution was aged and spray-dried under the same conditions as described above. The specimen obtained from this method was named aggregated casein micelle (ACM). The spray-dried

powders were kept in amber glass vials and were stored in a desiccator over silica gel until analysis.

3.2.3 Encapsulation efficiency measurement

Encapsulated β-carotene was extracted by using hexane. The dried powder (0.1 g) was dispersed in 10 mL of hexane and stirred for 5 min or 24 h at ambient temperature. The mixture was filtered by using a 0.45 μm membrane filter. The absorbance of the filtrate was measured using a U-5100 Ratio-Beam UV-visible spectrophotometer (Hitachi High-Technologies Corporation, Tokyo, Japan) at 450 nm. The absorbance of the extract sampled after 5 min was used to determine the amount of free β-carotene, and the extract sampled after 24 h was used to determine the total β-carotene load. The free β-carotene and encapsulation efficiency were calculated using the following equations:

$$\text{Free } \beta\text{-carotene} = \left[\frac{\text{Extracted amount of } \beta\text{-carotene after 5 min}}{\text{Total } \beta\text{-carotene load in the original solution}}\right] \times 100 \qquad (3\text{–}1)$$

$$\text{Encapsulation efficiency (Entrapped } \beta\text{-carotene)} = \left[\frac{\text{Extracted amount of } \beta\text{-carotene after 24 h} - \text{Free } \beta\text{-carotene}}{\text{Total } \beta\text{-carotene load in the original solution}}\right] \times 100 \qquad (3\text{–}2)$$

3.2.4 Stability

The dried powder (0.1) was spread in thin layers in 50 mL glass vials, which were then placed in desiccators at 60°C under the following storage conditions: 11% and 75% relative humidity (RH) using saturated salt solutions (lithium chloride and

sodium chloride, respectively). At selected time intervals, the sample vials were removed from the desiccators. The color changes of the dried samples were assessed using the tristimulus color coordinates (L^*, a^*, and b^*) by using an SA 4000 spectrophotometer (Nippon Denshoku Industries Co., Tokyo, Japan); the color change was used to estimate the degradation of β-carotene. Hexane extraction, described above, was also used to determine the remaining amount of β-carotene in the dried powder.

3.2.5 Characterization of casein clusters by SAXS

SAXS measurements were done at SPring-8, the same as described in 2.2.5, with a camera length of 4,139 mm. The sample solution (before spray-drying) was filled into a quartz capillary tube (diameter: 2 mm; wall thickness: 0.01 mm). The capillary tube was set on a sample holder and placed on the measurement stage.

3.3 Results and discussion

3.3.1 Encapsulation efficiency

The sample solutions were aged for 0, 24, 48, 72, and 120 h, and the aged samples were spray-dried to analyze the encapsulation efficiency. The encapsulation efficiency and free β-carotene content of specimen A70 were 54.4 ± 2.3% and 2.8 ± 0.3%, respectively (Figure 3–1A). These values did not change appreciably with aging. However, the encapsulation efficiency of A60 increased from 73.0% to 82.8% after 120 h of aging, and the free β-carotene content concomitantly decreased from 4.5% to 2.5% (Figure 3–1B). This result suggested that the structure of the aggregated casein formed under acidic conditions (pH 6.0) modifies during the aging period; this

deformation is linked to the entrapment of β-carotene. The increased encapsulation efficiency of A60 could thus be caused by the relocation of free β-carotene to the inner region of the casein cluster due to cluster deformation. However, lowering the solution pH also affected the surface hydrophobicity of casein. Previous studies showed that lowering the solution pH increased the surface hydrophobicity of casein and induced casein aggregation (Liu & Guo, 2008; Risso et al., 2008). Therefore, in this work, the encapsulation efficiency increased, probably because of the increase in the hydrophobic regions of the casein cluster under the low pH condition, and this mechanism may occur along with aging. No apparent effect of aging on the encapsulation properties of ACM was observed, and approximately constant encapsulation efficiency values were obtained despite aging; in contrast, the free β-carotene content continuously increased on aging (Figure 3–1C). Considering that the sum of the encapsulation efficiency and free β-carotene (58.1 ± 3.2%) did not vary with aging, the increase in the free β-carotene content may be attributed to the collapse of the micellar structure during aging.

3.3.2 β-Carotene retention and color change during storage

The retention of β-carotene in the spray-dried powder was determined by measuring the remaining amounts of β-carotene during storage under constant humidity (i.e., 11%RH or 75%RH) at 60°C. When the powders were prepared without aging, the retention rapidly declined in the initial 14 d under 11%RH and within 3 d under 75%RH, and subsequently decreased slowly. The decline in the retention with time was obviously higher at higher relative humidity during the first two weeks of

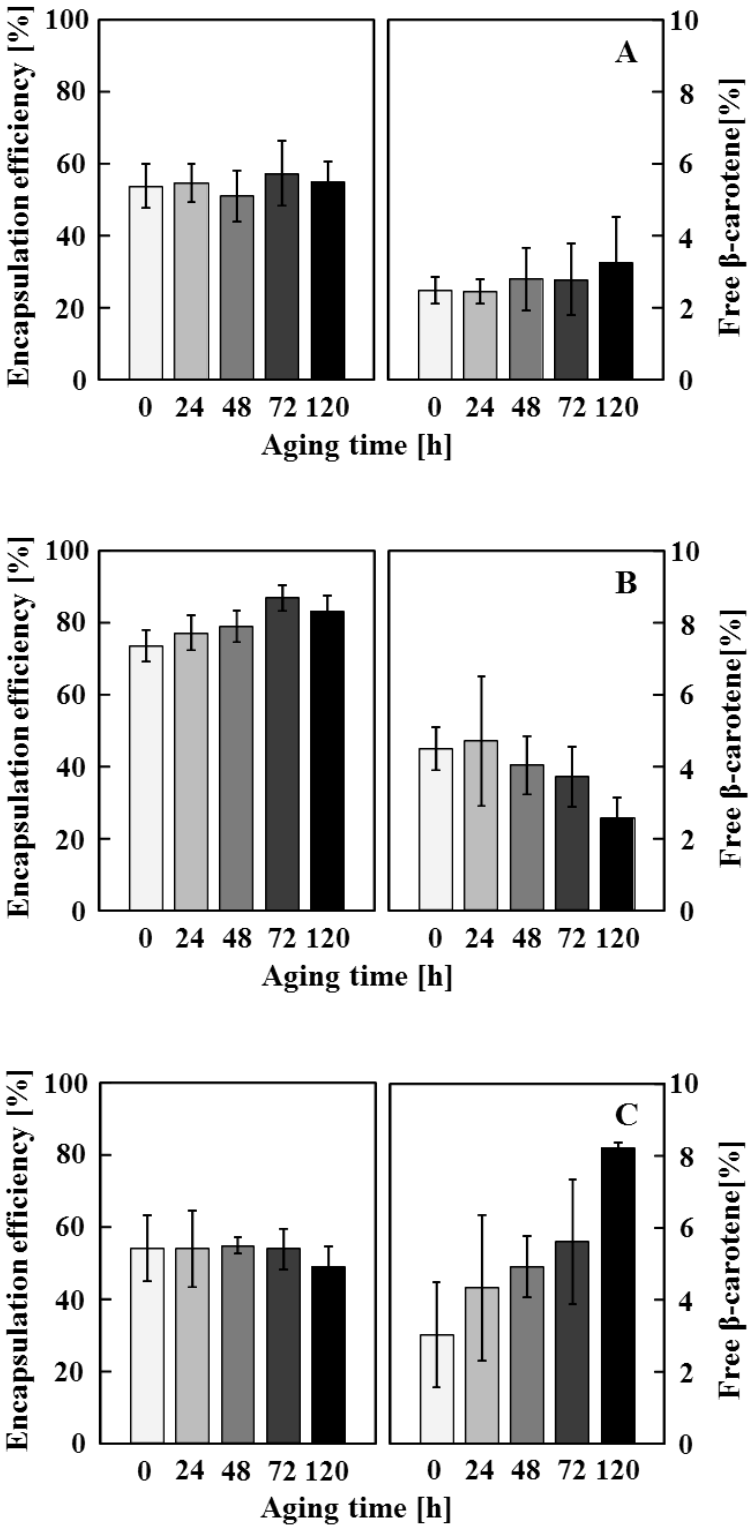

Figure 3–1: Encapsulation efficiency and free β-carotene as a function of aging time: (A) A70; (B) A60; (C) ACM (error bars represent SD, $n = 3$).

storage (Figure 3–2A and B). The significant degradation of β-carotene at 75%RH may be attributed to the collapse of the cluster structure due to moisture sorption. Sixty percent of β-carotene was lost from ACM within one week under 11%RH, and 80% loss was observed under 75%RH; in contrast, 60% of β-carotene was retained by A60 under 11%RH and 40% was retained under 75%RH in the same period. The retention of β-carotene for all samples was reduced to less than 10% in 21 d, and the amount of β-carotene retained in A70, A60, and ACM was largely similar at the final stage.

The surface color changes of the prepared powders were evaluated in terms of the total color difference (ΔE^*), which can be used as an indicator of overall color fading due to β-carotene degradation (Desobry et al., 1997; Qian et al., 2012).

$$\Delta E^* = [(L^* - L_0^*)^2 + (a^* - a_0^*)^2 + (b^* - b_0^*)^2]^{1/2} \quad (3\text{–}3)$$

where L_0^*, a_0^*, and b_0^* are the initial color coordinates of the sample powder.

The fresh, spray-dried powder had a light orange color that gradually faded to white during storage. This color fading reflects chemical degradation of β-carotene. Under 11 and 75%RH, the ΔE^* value of the dried powders increased linearly as a function of storage time, and a greater degree of color change was confirmed for the sample stored at higher relative humidity (Figure 3–2C and D). The large ΔE^* value observed with A60 could be due to the large amount of free β-carotene. As seen in the previous section, the amount of free β-carotene for A60 could be reduced by aging; thus, it is expected that this feature changed the retention of β-carotene.

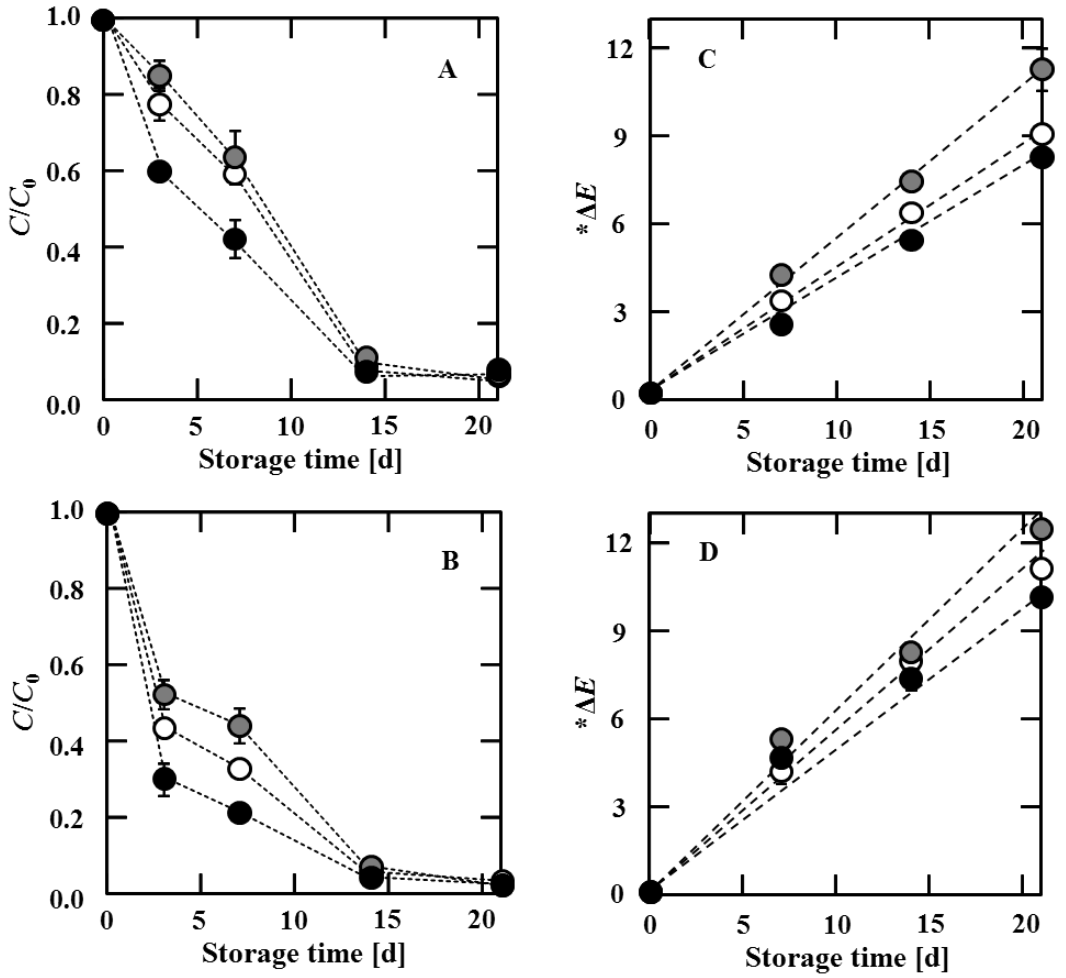

Figure 3–2: Retention of encapsulated β-carotene under 11%RH (A) and 75%RH (B); and surface color changes under 11%RH (C) and 75%RH (D) of A70 (○), A60 (◍), and ACM (●) as a function of storage time at 60°C (error bars represent SD, n = 3).

The retention of β-carotene in the non-aged and 120-h aged specimens is compared in Figure 3–3A, B, and C. The β-carotene retention of the 120-h aged specimens was higher than that of the non-aged sample, even under high relative humidity. As discussed above, >90% loss of β-carotene from A70 and A60 was observed after storage under 75%RH for 14 d, whereas 25.2% and 29.6% β-carotene

retention values were respectively observed for 120-h aged specimens of A70 and A60 under similar storage conditions. However, the influence of aging on the stability at low relative humidity was not significant. On the other hand, the stability of ACM improved after 120 h of aging under low as well as high relative humidity (Figure 3–3C). Aging also affected the color change of the resultant powders. The rate of variation of the ΔE^* value for A70 and A60 reduced when the specimens were aged for 120 h. Interestingly, the total color change was less when the samples were stored under high relative humidity (Figure 3–3D and E). At the end of 20 d storage, the ΔE^* values for A70 and A60 were 11.06 and 12.40, respectively, whereas those for the aged specimens were 4.95 for A70 and 7.50 for A60. However, aging did not influence the color change of the specimens prepared using ACM (Figure 3–3F).

3.3.3 Structural and morphological characterization

The scattering profiles for A70, A60, and ACM, which were prepared from 5% SC solution without dilution, are compared in Figure 3–4A. The relative difference in each scattering curve indicates differences in the microstructure of the clusters. The peaks around $q \approx 0.1–0.3$ nm^{-1} correspond to the inter-particle distance, though the peaks themselves do not reflect any structural features of the clusters. These peaks are the so-called Bragg peaks and the peak position (q_{peak}) indicates the distance between the aligned particles (d_{Bragg}) based on Bragg's law: $d_{Bragg} = 2\pi/q_{peak}$ (Bassett, 1981; Fiori & Spinozzi, 2010). The d_{Bragg} values of A70, A60, and ACM were approximately 23.7, 29.0, and 31.0 nm^{-1}, respectively. With decreasing pH, the d_{Bragg} value of the casein aggregates increased; this means that the mean intra-particle

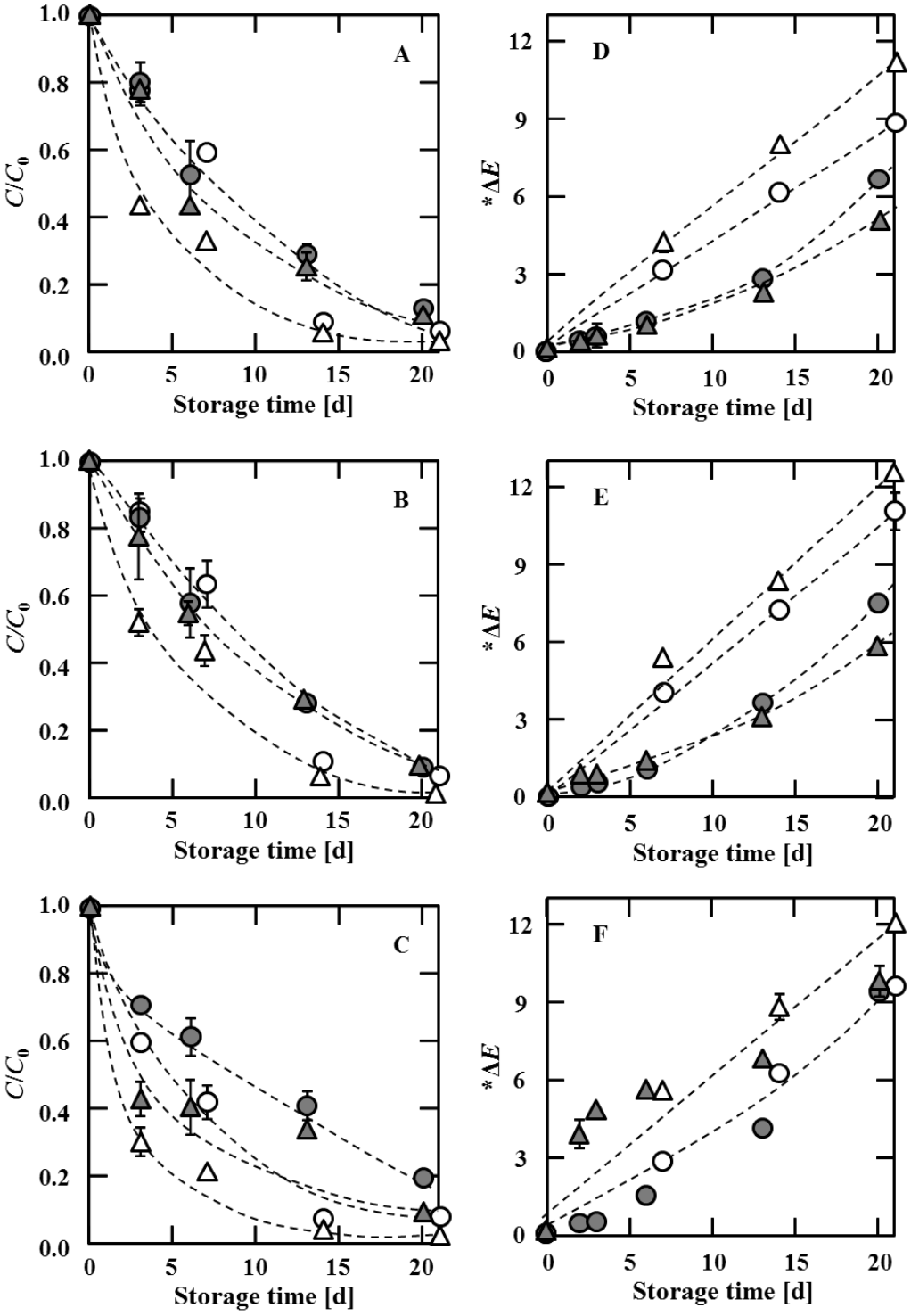

Figure 3–3: Retention of encapsulated β-carotene in A70 (A), A60 (B), and ACM (C) and surface color changes of A70 (D), A60 (E), and ACM (F) under 11%RH (non-aged (○) and 120-h aged (●)) and 75%RH (non-aged (△) and 120-h aged (▲)) as a function of storage time at 60°C (error bars represent SD, $n = 3$).

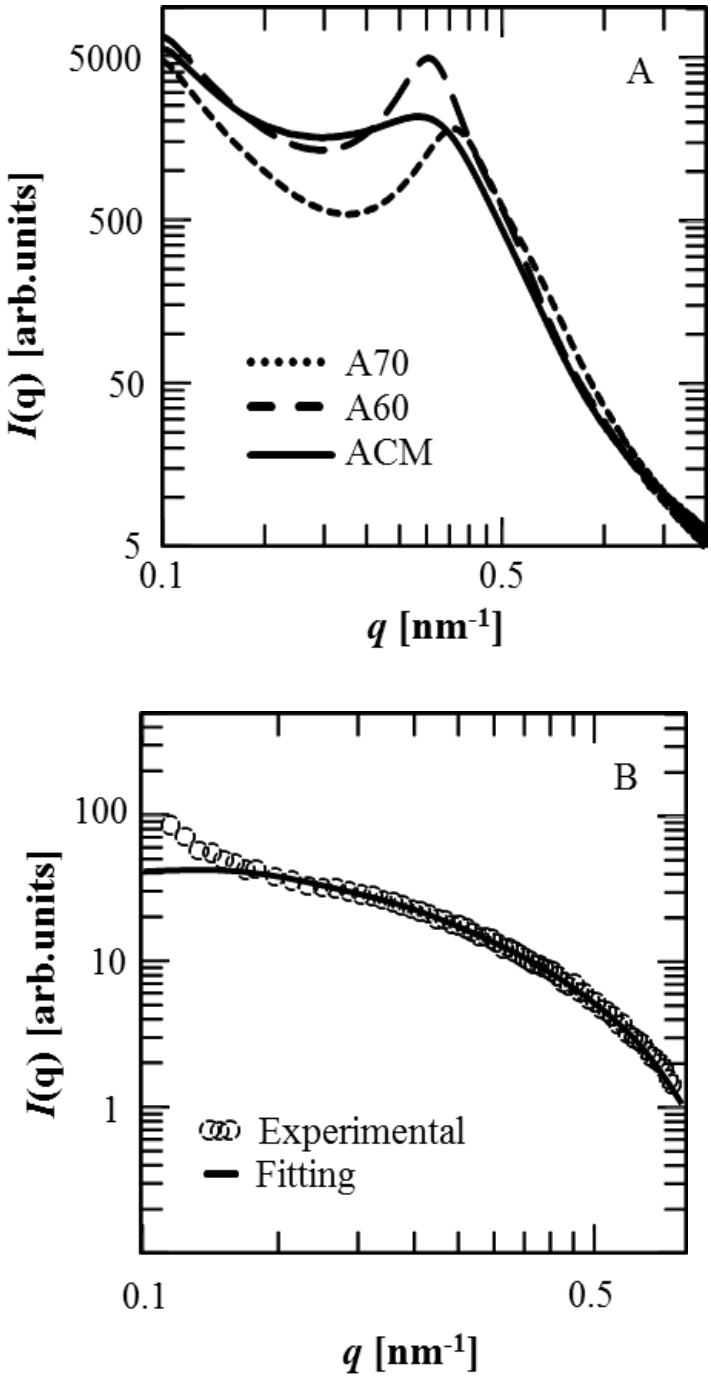

Figure 3–4: SAXS profiles obtained from 5% specimen solutions (A) and SAXS profiles of 0.1% A60 (B).

distance increased and the probability of finding a next-neighbour particle at a specific distance decreased. The difference in the peak position for the A70, A60, and ACM samples suggested differences in the numbers of proteins associated with the aggregates. The scattering pattern of ACM was notably different from those of A70 and A60, suggesting differences in the nano- and micro-structures.

For evaluating radius of gyration (R_G) and zero angle intensity ($I(0)$), the scattering data were measured by using the diluted specimen solution (0.1% w/v) to avoid the effect of the neighbour particles. Figure 3–4B shows the scattering profile of A60, which was fitted by following the model equation for the scattering function (described in 1.3). The R_G values for A70, A60, and ACM were 6.42, 6.76, and 5.89 nm, respectively, and the D values were approximately 3.1 for all specimens. These values suggest that the obtained casein clusters were fractal with rough surface and the cluster prepared by the aggregation system was larger than that prepared from the reassembled system. Previous studies reported that the casein micelles were aggregated and formed a fractal structure by acidification (Bremer, 1989; Chardot et al., 2002). Dziuba et al. (1999) investigated the fractal dimension of acid casein and caseinate obtained from various preparations using image analysis. Their results suggested that fractal characteristics as well as the particles size of casein were dependent on their chemical composition caused by the preparations. Although the casein clusters in A60 and ACM were similar in size, they were different in density, i.e., the density index values (δ) for A60 and ACM were 0.13 and 0.09 nm^{-3}, respectively. This is consistent with the results of TEM observation shown in Figure 3–5. ACM formed a cluster with randomly grown branches in stelliform geometry,

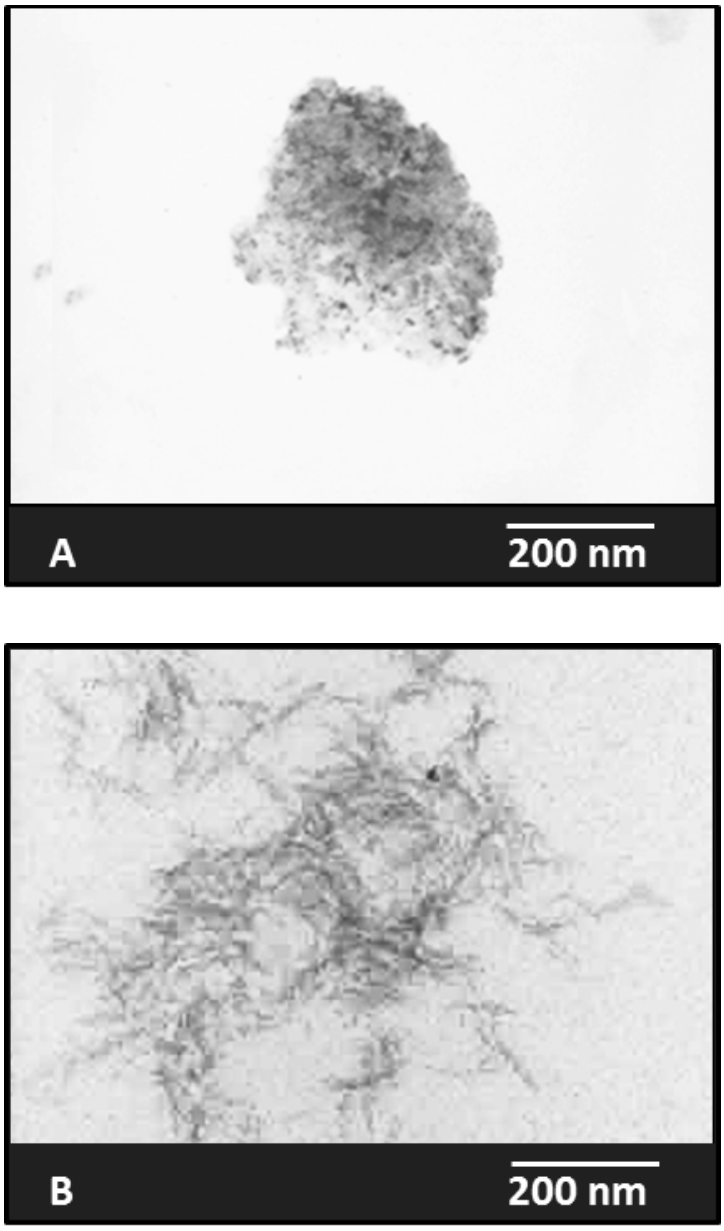

Figure 3–5: TEM images of rehydrated specimen powder: A60 (A); ACM (B).

and each cluster comprised a number of small cylindrical units (Figure 3–5B). These nano- and microstructures were obviously different from the packed structures in the aggregated casein clusters (Figure 3–5A). Based on the β-carotene retention analysis, the significant loss of β-carotene from ACM corresponds to the data obtained from the SAXS and TEM analyses. The ACM cluster consisted of small aggregated

particles and its density was possibly lower than that of A60. It is plausible that this type of structure is not suitable for maintaining the stability of loaded substances in the dried form.

Figure 3–6 shows the scattering profiles, R_G, and δ values of the specimens in solution plotted as a function of the aging time. The influence of aging on the nanostructure of casein cluster was different due to cluster preparation. In the case of A70, the R_G values gradually decreased, while the δ values increased over the stated time course. Moreover, aging the A70 specimen solution increased the D value from 3.08 to 3.42. This suggests that the surface of A70 cluster became smoother with reduction in cluster size and increase in cluster density during aging, probably because of the elimination of some small branches at the cluster surface (Figure 3–6A).

In the case of A60, the R_G values increased, whereas the δ values were rather constant. From these observations, it is deduced that dense and packed clusters were formed by aggregation, induced by acidic conditions; the clusters then slowly underwent further aggregation and maintained their cluster density. Similar to A70, the cluster of A60 would lose unstable branches during aging, resulting in a smoother surface, as confirmed by the increase in D values from 3.0 to 3.51 during 120 h of aging (Figure 3–6B). However, the trend of the change in the cluster structure of ACM was different; the clusters grew with decrease in both the cluster density and D values (from 3.26 to 2.99). This suggests that the ACM clusters grew by maintaining

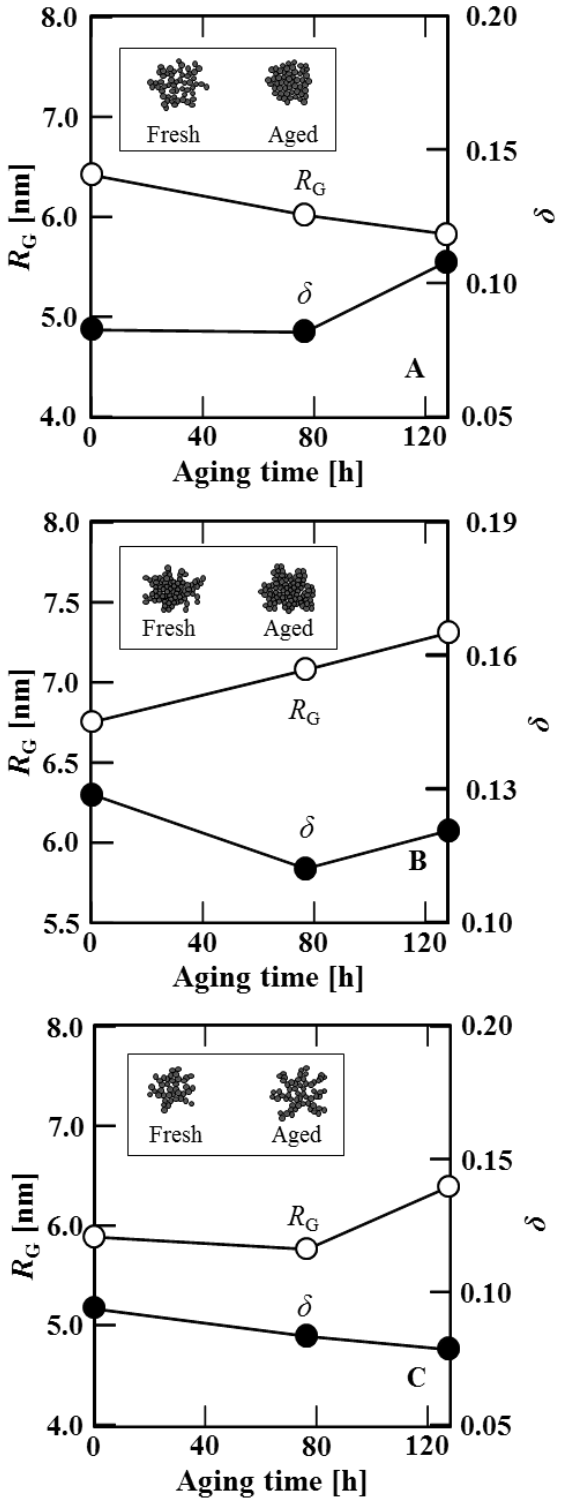

Figure 3–6: Radius of gyration (R_G), density index (δ), and illustrations of fresh and aged cluster (inset) for A70 (A), A60 (B), and ACM (C) as a function of aging time.

the hollow and branched structure (Figure 3–6C). This hollow structure of ACM seems much weaker than the packed structure of A70 and A60. Therefore, it can be easily broken during spray-drying, thus increasing the free β-carotene content. As discussed in the previous section, when powders were prepared using A60, the encapsulation properties were found to be related to the deformation of the clusters during aging. The observed deformation is due to the aggregate growth, as observed in the SAXS analysis. This suggests that the stability and encapsulation efficiency of the spray-dried powders were closely linked to the nanostructures of the original clusters.

3.4 Conclusions

Two types of casein clusters, aggregated casein and re-assembled casein micelles, were prepared for stabilizing β-carotene by hydrophobic interactions. The prepared solutions were aged under ambient conditions and spray-dried. The encapsulation efficiency of the aggregated casein was higher than that of the re-assembled casein micelles, and aggregated casein prepared at pH 6.0 had the highest encapsulation efficiency. Aging of aggregated casein prepared at pH 6.0 was effective for improving the encapsulation efficiency and reducing the amount of free β-carotene. However, aging of dried re-assembled casein micelles did not improve the encapsulation efficiency. Evaluation of the dried powders after storage demonstrated that aging improved the storage stability of the dried powders; this trend was most obvious for the specimens prepared from aggregated casein at pH 6.0. Moreover, the change in the cluster structure during aging was clearly observed with the aggregated casein solution at pH 6.0. This change may be an evidence of the structural

deformation of aggregated casein clusters, suggesting that the cluster slowly aggregated to form a stable structure. This deformation is significant for the entrapment of β-carotene stabilized with casein via hydrophobic interactions.

Chapter 4

Digestibility and structural parameters of spray-dried casein clusters under simulated gastric conditions

4.1 Introduction

The digestibility of encapsulants (wall materials) in the gastrointestinal tract is a key factor that affects the functionality of microcapsules. Numerous studies have reported the release characteristics and digestibility of microcapsules under simulated gastric digestion conditions *in vitro*. The attributes of the wall materials, such as composition, shape, size, surface charge, and hydrophobicity, have a crucial effect on digestibility (McClements & Li, 2010; Shapira et al., 2012; Singh & Ye, 2013; Flores et al., 2015; Liu et al., 2015). Augustin et al. (2014) showed that the *in vitro* digestibility of microencapsulated oil powders was dependent on the protein composition and processing conditions. Ao and Li (2013) reported the difference in digestive resistance between the positively and negatively charged fractions of alcalase-treated casein hydrolysate. The negatively charged fractions were the most stable, and the antioxidant activity of the encapsulated substances was retained during digestion. Burgain et al. (2013) and Zhang and Vardhanabhuti (2014) emphasized the effect of structural changes under gastric conditions on digestive resistance.

This chapter aims to investigate the nano and microstructures of the pH induced casein clusters spray-dried at different drying temperatures. This is to clarify how the drying temperature affects the cluster structures that would relate to their

encapsulation efficiency and digestibility. A simulated digestion test was carried out to analyze digestion kinetics and structural changes during digestion by using small angle X-ray scattering technique.

4.2 Materials and methods

4.2.1 Materials

Sodium acetate, hydrochloric acid, sodium tetrahydroborate, dimethyl sulfoxide (DMSO), 1-anilinonaphthalene-8-sulfonic acid (ANS), and trichloroacetic acid (TCA) were purchased from Wako Pure Chemical Industries, Osaka, Japan. All other chemicals were the same as described in 2.2.1.

4.2.2 Particle preparation

The preparation of sample solution was done in the same method described in 3.2.2. The prepared solution was dried with the different inlet air temperature. The operational conditions (i.e. inlet air temperature, outlet air temperature, feed flow rate, and atomizer rotational speed) were adjusted according to the inlet air temperature and are described in Table 4–1. The obtained powders were stored in a desiccator for further analysis.

Table 4–1 Specimen details and spray-drying conditions.

Specimen IDs	Preparation conditions	Inlet air temperature [°C]	Outlet air temperature [°C]	Feed flow rate [mL/min]	Rotational speed of atomizer [rpm]
A70-150	Without pH adjustment	150	110 ± 5	20	5000
A60-150	pH adjusted to 6.0				
A70-180	Without pH adjustment	180	126 ± 5	25	5000
A60-180	pH adjusted to 6.0				

4.2.3 Encapsulation efficiency measurement

The amount of entrapped β-carotene and the EE of dried specimens were analysed and determined by the same methods described in 3.2.3.

4.2.4 Surface hydrophobicity measurement

An ANS hydrophobic fluorescence probe was used to determine the surface hydrophobicity (SH) of the dried casein clusters, following the procedure described by Hayakawa and Nakai (1985) with slight modifications. A series of specimen solutions with concentrations ranging from 0.0005% to 0.01% (w/v) were prepared by diluting the prepared sample (before spray-drying) or dissolving dried casein clusters in 0.05 mol/L phosphate buffer at pH 7.0. ANS solution (25 μL of 8 mmol/L ANS in 0.05 mol/L phosphate buffer) was added to 5 mL of the specimen solution. The fluorescence intensity (FI) of the mixture was measured using a spectrofluorophotometer (RF-1500, Shimadzu Corporation, Kyoto, Japan) with excitation and emission wavelengths of 390 nm and 470 nm, respectively. The

relative fluorescence intensity (RFI) of each specimen concentration was determined by subtracting the FI of the control specimen solution (25 μL of 0.05 mol/L phosphate buffer was added instead of ANS). The SH index was obtained from the initial slope of the RFI versus the specimen concentration (% (w/v)).

4.2.5 Simulated gastric digestion

The simulated digestion method described by Mandalari et al. (2009) was used with modifications to estimate the digestibility of the dried casein clusters. Dried casein clusters (0.1 g) were dissolved in 10 mL of the simulated gastric fluid (SGF; pH 2.0 HCl solutions). The mixture was stirred for 2 h to ensure complete dissolution. Pepsin in SGF (5 mg/mL) and protein solution were incubated at 37°C in a thermostatic bath for 10 min prior to the reaction starting. Pepsin solution (1 mL) was added to the mixture to give a pepsin: dried casein cluster ratio of 1:20 (w:w). To study the digestion behaviour, 0.6-mL aliquots of the digested solution were collected at predetermined intervals, and the reaction was stopped by adding a mixture of 0.05 mol/L phosphate buffer and 0.1 mol/L NaOH to adjust the pH to 6.0. This digested solution was used immediately for further analyses.

4.2.6 Estimation of digestion kinetics

The amounts of amino acids produced by digestion were determined using the ninhydrin reaction according to the method described by Takahashi (1978) with modifications. Ninhydrin solution was prepared by dissolving 29.5 mg of $NaBH_4$ in 300 mL of 0.15 mol/L ninhydrin in DMSO. The digested casein solution (0.5 mL) was mixed with 0.5 mL of 5% (w/v) TCA to precipitate large peptides and undigested

proteins; thus, small peptides and amino acids were detected. After incubation at ambient temperature for 10 min, the mixture was centrifuged at 5,000 rpm for 10 min. The supernatant (200 μL) was added to a mixture of 600 μL of ninhydrin solution and 200 μL of 0.4 mol/L sodium acetate buffer with a pH of 5.0. The mixture was incubated in a thermostatic bath at 80°C for 30 min. The amino acid concentration was estimated by measuring the absorbance at 570 nm with a U-5100 spectrophotometer, using leucine solution as the standard. The percentage of digested casein was calculated using the following equation:

$$\text{Digested casein}\,[\%] = \frac{\text{Amount of amino acid produced during digestion}}{\text{Amount of total digested casein}} \times 100 \quad (4\text{–}1)$$

where the amount of total digested casein was determined from the complete hydrolysis of casein by heating for 24 h at 105°C with HCl solution of pH 2.0 in a tightly sealed vial.

4.2.7 Characterization of casein clusters by SAXS and USAXS

The structural characteristics of casein clusters during digestion were analyzed by SAXS and USAXS. The digestion process for the measurement was separated into several steps, namely; the rehydration step (casein powder was dissolved in distilled water at 1% (w/v)), the initial step (casein powder was dissolved in SGF at 1% (w/v)), and the digestion step (pepsin was added to the SGF containing the dissolved casein powder).

SAXS measurements were done at SPring-8, the same as described in 2.2.5, with a camera length of 4,139 mm. USAXS measurements were performed at the BL19B2 beamline, which is a bending magnet beamline with a long path camera. X-ray energy of 18 keV and camera length of 41,649 mm, which correlates with the q range of 0.003–0.1 nm^{-1}, were used. For both the measurements, the test solution was filled into a quartz capillary tube (diameter: 2 mm, wall thickness: 0.01 mm) and placed on the sample stage.

4.3 Results and discussion

4.3.1 Encapsulation efficiency and surface hydrophobicity

The encapsulation efficiency of the present specimens varied between 45–73%, and it was apparent that the A60 specimens were superior to the A70 specimens. The amount of β-carotene loaded in specimens A70 and A60 reduced by approximately 9% and 4%, respectively, owing to the increase in the spray-drying temperature from 150°C to 180°C (Figure 4–1A). This finding is in accordance with the previous researches (Goula & Adamopoulos, 2005; Quek et al., 2007; Tuyen et al., 2010). They reported that the significant loss of the entrapped materials mainly caused by thermal degradation and oxidation. Interestingly, Shu et al. (2006) reported that high inlet air temperature could disrupt the balance between the water evaporation rate and film-formation of microcapsules. This caused the stability and encapsulation yield of dried powder.

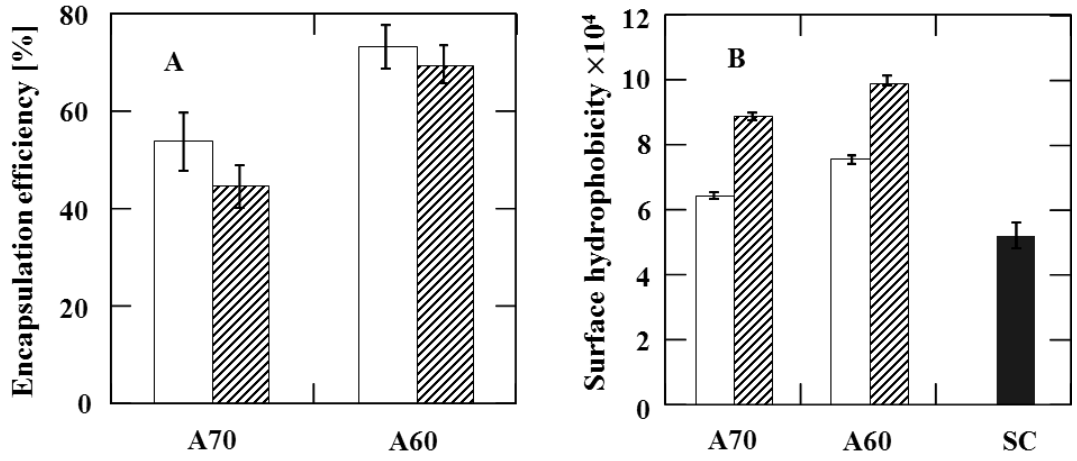

Figure 4–1: Encapsulation efficiency (A) and surface hydrophobicity (B) obtained from the specimens spray-dried at 150°C (□) and 180°C (▨), (error bars represent SD, *n*=3).

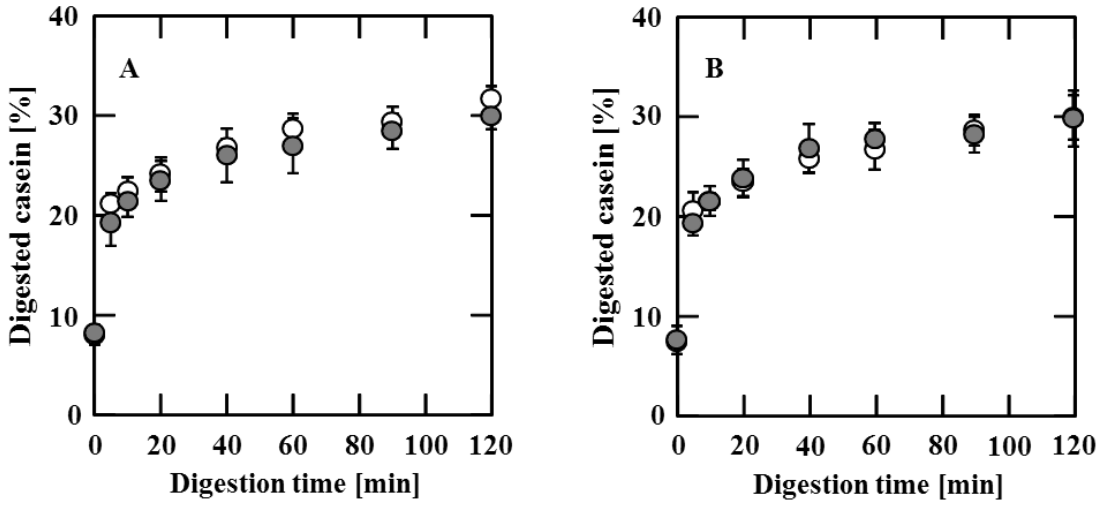

Figure 4–2: The amount of digested casein as a function of digestion time obtained from the specimens (A70 [○] and A60 [●]) spray-dried at 150°C (A) and 180°C (B), (error bars represent SD, *n*=3).

On the contrary, several studies showed that the increase in drying temperature had no significant effect on the encapsulation efficiency as well as the encapsulation rate, although obvious changes in the moisture content and surface morphology of dried powders were observed (Roccia et al., 2014; Ixtaina et al., 2015; Pai et al., 2015). According to our previous study, the structure of the casein clusters is dependent on the preparation conditions (Nakagawa et al., 2014). When the pH was adjusted before drying, the casein clusters were primarily formed in the prepared solution and effectively entrapped β-carotene. However, cluster formation in the plain solution was scarce, and hence, the entrapment mainly occurred in the drying step. The present results demonstrate that the formation of casein clusters in A60 could strongly protect β-carotene against spray drying, whereas the entrapment of β-carotene in A70 would be induced by the drying step.

The heat during drying could cause protein denaturation. Numbers of researchers have been reported the effect of heat on the stability of casein. For example, Sauer and Moraru (2012) reported that the micellar caseins lost their stability and the aggregation occurred when they were heated at 110 and 150°C under the pH lower than 6.7. The aggregation was also observed in the heated β-casein (Farrell et al., 2002). The structure of heated β-casein was different depending on the temperature used (Qi et al., 2004). Usually, heating affects the hydrophobic sites of proteins, resulted in protein aggregates via hydrophobic interactions. This aggregation is strongly related to the surface hydrophobicity and the protein denaturation (Yüksel & Erdem, 2005; Yazdi & Corredig, 2012). The SH measurement probed by ANS is one of a simple method that can be used to evaluate the protein denaturation (Nakai,

1983; Hayakawa & Nakai, 1985; Alizadeh-Pasdar & Li-Chan, 2000). The measured SH values of solutions before drying and rehydrated dried specimens are compared in Figure 4–1B. The SH values observed in A60 solution was slightly higher than that of A70. These values increased obviously when the specimens were spray-dried, suggesting that casein cluster was denatured to a certain extent by pH adjustment and during drying. The higher drying temperature caused an increase in the SH, and the level of the effect was dependent on the type of casein cluster. A larger difference in the SH values was observed in A70, approximately 27% increase, compared to A60 (23%). It was reported that a heat-induced rise in SH was observed in milk proteins, and it was caused by the denaturation of their tertiary and secondary structures (Eynard et al., 1992; Sava et al., 2005; Euston et al., 2007; Risso et al., 2008). When adjusting the pH of a milk protein solution, the change in SH value was observed to be closely link with their solubility and functional properties (Voutsinas et al., 1983; Shimizu et al., 1985; Alizadeh-Pasdar & Li-Chan, 2000). Hence, in the present case, the change in SH is not only caused by the thermal stress during drying, but also the structural characteristics of the casein clusters.

4.3.2 Digestibility

The digestion profiles of the specimens dried at 150°C are compared in Figure 4–2A. The amount of digested casein increased rapidly in the first 40 min, followed by a gradual increase until 120 min of digestion. However, the effect of drying temperature on the amount of digested casein was not significant, as evidenced by digestion profile comparison of the specimens dried at 150°C to 180°C (Figure 4–2B). This study demonstrated that about 30% (by weight) of the casein clusters

were digested after 120 min of digestion. IInglingstad et al. (2010) reported that around 30% of bovine casein was broken down within 30 min of gastric digestion, whereas the majority was degraded within 5 min of duodenal digestion. During gastric digestion, the protein particles are broken down into peptides of various sizes owing to acid hydrolysis and pepsin proteolysis (Dupont et al., 2010; Mackie & Macierzanka, 2010). Agudelo et al. (2004) reported that casein was hydrolyzed into peptides with molecular weights exceeded 10 kDa after 30 min of pepsin hydrolysis. The denaturation of proteins by heat and chemical modifications affects the digestion of the peptide bond by pepsin (Singh & Ye, 2013). However, in other studies it has been reported that the digestion of milk casein was different depending on the method used such as batch or a dynamic digestion (Guri et al., 2014), enzyme used (Shanmugam et al., 2015) and the types of milk casein (Inglingstad et al., 2010). In present study, the observed amount of digested casein, about 30%, means the casein clusters would not largely be digested in stomach, and delivered to the subsequent intestinal tract. The most of the β-carotene associated with the clusters may be protected under gastric conditions and this will improve the bioavailability of β-carotene.

4.3.3 Characterization of casein clusters

The SAXS and USAXS profiles of specimens A70 and A60 at the rehydration step are shown in Figure 4–3A. For the lower q region, the scattering profile trends were similar for all specimens. An obvious difference in the scattering intensities could be observed between A70 and A60 in the higher q region. However, the influence of drying temperature on the scattering profile was not significant. The

structural parameters calculated from the scattering data are listed in Table 4–2. For the lower *q* region, the average size of the whole cluster (R_G^L) for all specimens was about 428 nm. The obtained D^L value (~3.2) suggested that the present clusters had a rough and fractal surface. The data obtained from higher *q* region that reflect the structures of the primary clusters, suggested a mass fractal structure with R_G^H within the range of 5.4 – 6.5 nm. These results suggested that the loosely assembled casein clusters were made up of many small dense clusters, as illustrated in Figure 4–3B. The cluster size of A70 was smaller than A60 both for the whole and primary clusters. The increased drying temperature resulted in an increase in their whole cluster sizes, whereas no significant change could be observed in the primary cluster. This change could be ascribed to the increase in the SH value that was related to the degree of denaturation, as discussed in the previous section. However, the influence of drying temperature on the *D* and δ values was not significant.

When specimens were dissolved in SGF (the initial step), their cluster structures are largely different from that observed in the rehydration step (Table 4–2). For A70-150 and A70-180, the R_G^L values were slightly larger than those observed during the rehydration step, while the R_G^L values for A60-150 and A60-180 were clearly larger than that in the rehydration step. Nevertheless, the trends of the changes in the primary cluster structures were quite similar for all specimens, where the R_G^L values doubled and the D^H values decreased. Interestingly, the δ^L and δ^H values dramatically

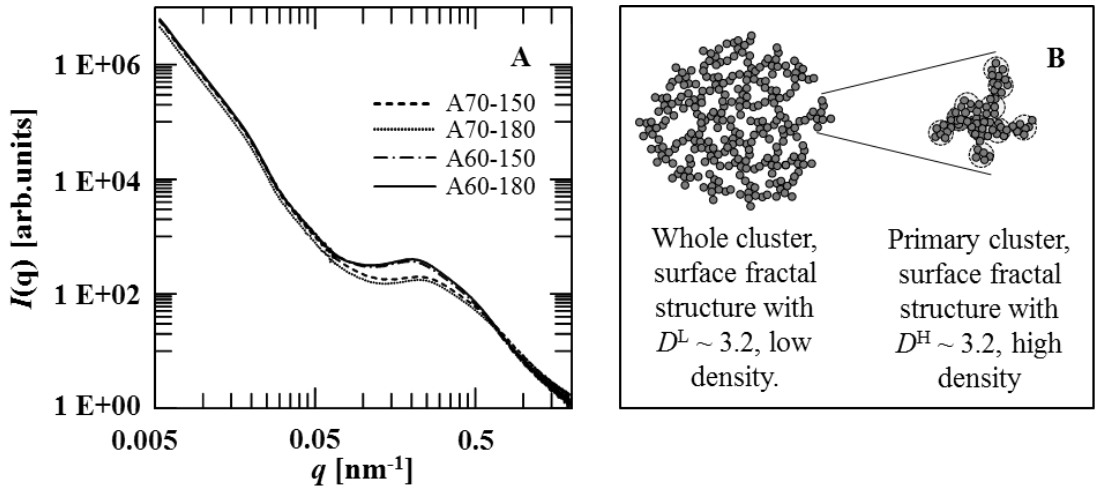

Figure 4–3: Combination of ultra-small-angle X-ray scattering (USAXS) and small-angle X-ray scattering (SAXS) profiles (A) and an illustration of casein cluster (B). D^{L}: fractal dimension obtained from the lower q region; D^{H}: fractal dimension obtained from the higher q region.

Table 4–2 Structural parameters of the casein clusters dissolved in distilled water and simulated gastric fluid (SGF).

		Lower q region			Higher q region		
		R_G^L [nm]	D^L	δ^L [nm^{-3}]	R_G^H [nm]	D^H	δ^H [nm^{-3}]
In distilled water	A70-150	385	3.2	1.72×10^{-4}	5.4	3.0	2.06
	A70-180	404	3.2	1.74×10^{-4}	5.4	3.1	1.82
	A60-150	426	3.2	1.78×10^{-4}	6.5	3.2	2.24
	A60-180	499	3.3	1.75×10^{-4}	6.3	3.3	2.65
In SGF	A70-150	414	3.2	1.49×10^{-5}	11.3	2.5	0.30
	A70-180	408	3.2	1.51×10^{-5}	9.9	2.5	0.32
	A60-150	939	2.9	1.49×10^{-5}	12.3	2.4	0.31
	A60-180	519	3.1	1.48×10^{-5}	11.0	2.5	0.35

decreased in SGF. These results suggest that the clusters exhibit a significantly different formation in SGF compared to that in distilled water, that is, less dense and not very large clusters made up of larger primary clusters. The present results are supported by former studies on the aggregation of casein clusters when dispersed in gastric solution (Burgain et al., 2013; Qi et al., 2007).

In the digestion step, the obvious difference in the whole cluster structure of A70 can be seen in the first 20 min of digestion (Figure 4–4). The R_G^L increased about twofold for A70-150 and about threefold for A70-180 (Figure 4–4A). The fractal characteristic changed from surface fractals to mass fractals, that is, the D^L decreased from 3.2 to 2.8. The δ values slightly decreased at the beginning of digestion, and then remained constant for both A70-150 and A70-180 (Figure 4–4B). The primary cluster size increased as the digestion progressed, while the D^H value decreased slightly at the beginning of digestion. Moreover, the δ value decreased approximately 10-fold lower than that in the initial step (Figure 4–4C and D). It was apparent that the drying temperature affected the cluster sizes during digestion, namely R_G^L and R_G^H. A higher drying temperature led to a smaller R_G^L and a larger R_G^H.

The changes in the structural parameters during the digestion of A60 are summarized in Figure 4–5. The major structural changes occurred in the first 20 min of A60 digestion similar to A70, and the trends for the parameter changes were similar to A70, that is, the D^H and the δ values decreased (Figure 4–5D). The increase

in the cluster size and the decrease in the D^{L} value provide evidence for cluster aggregation during digestion (Figure 4–5A and B). The drying temperature affected the primary cluster size, R_{G}^{H}, during digestion, whereas it did not affect the whole cluster size, R_{G}^{L}. The higher drying temperature led to a larger R_{G}^{L}, an effect contrary to that observed for A70.

In this study, the changes in the cluster structure of casein can be recognized with 3 major steps. At the initial step (rehydrated in SGF), the increase of cluster size in this step could be explained by the aggregation that induced by acidic conditions and the degree of aggregation was related to the hydrophobicity. At the beginning of digestion step, the increase in cluster size still occurred with an obvious decrease in the density of primary cluster. Considering with the digestibility discussed in the previous section, approximately 30% of casein was digested; this may come from the reaction at the surface of the cluster that evidenced in the decrease of the *D* values, which reflects a change in the surface morphologies. Li et al. (2012) reported that the proteolysis of the casein-emulsion droplets occurred at the surface, and that it was related to the change in droplet size and microstructure. A major structural change would thus occur in this beginning step, where proteolytic products contribute to increasing the whole cluster size and reducing the primary cluster density with the formation of a rough and fractal surface. In the subsequent digestion step, digestion proceeded with only moderate structural changes, where the size of the primary cluster increased without changing the whole cluster sizes. This corresponded well with the digestion profiles that the amount of digested casein increased rapidly only at the beginning. The spray-drying temperature affected the resultant digestibility of the

casein clusters, and the influence was mainly apparent on the primary cluster sizes. With further investigation, this information could be useful for designing protein-based encapsulation systems with high bioavailability.

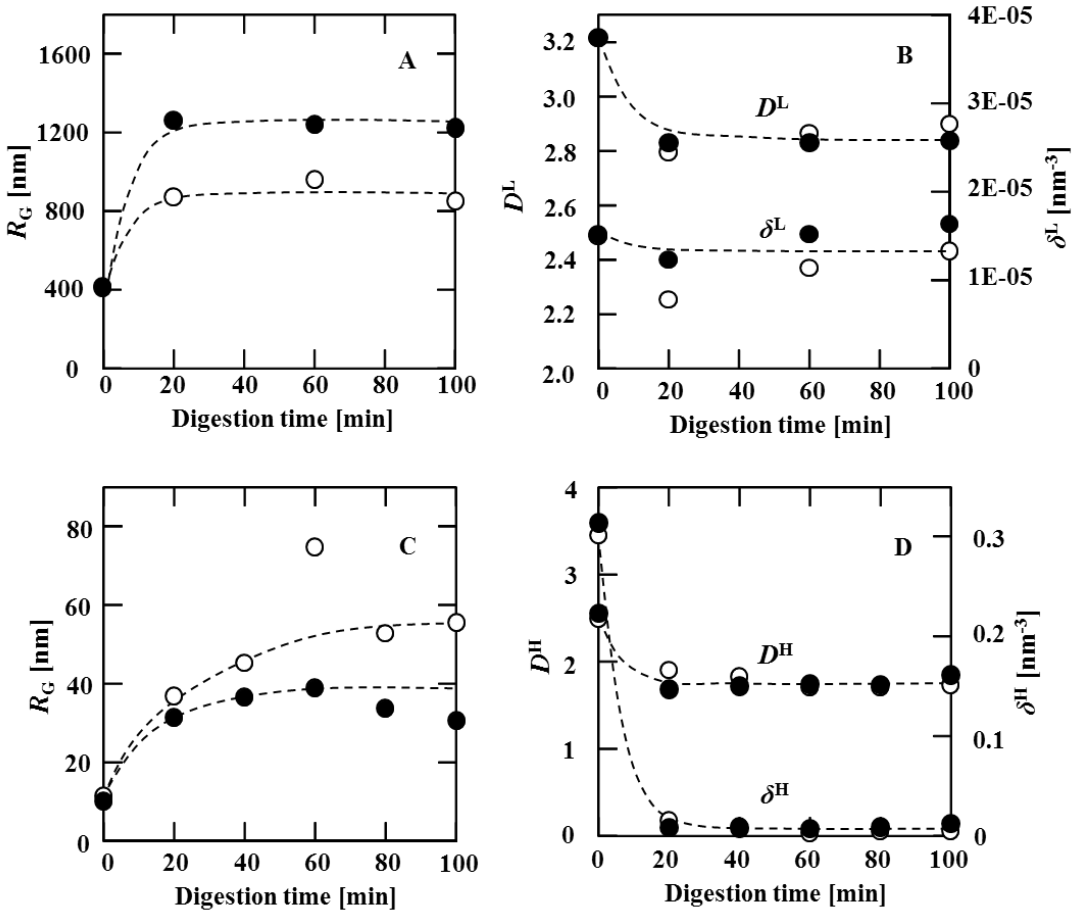

Figure 4–4: The structural parameters for A70-150 (○) and A70-180 (●): radius of gyration (R_G^L) obtained from the lower q region (A); fractal dimension (D^L) and density index (δ^L) obtained from the lower q region (B); radius of gyration (R_G^H) obtained from the higher q region (C); and the fractal dimension (D^H) and density index (δ^H) obtained from the higher q region (D).

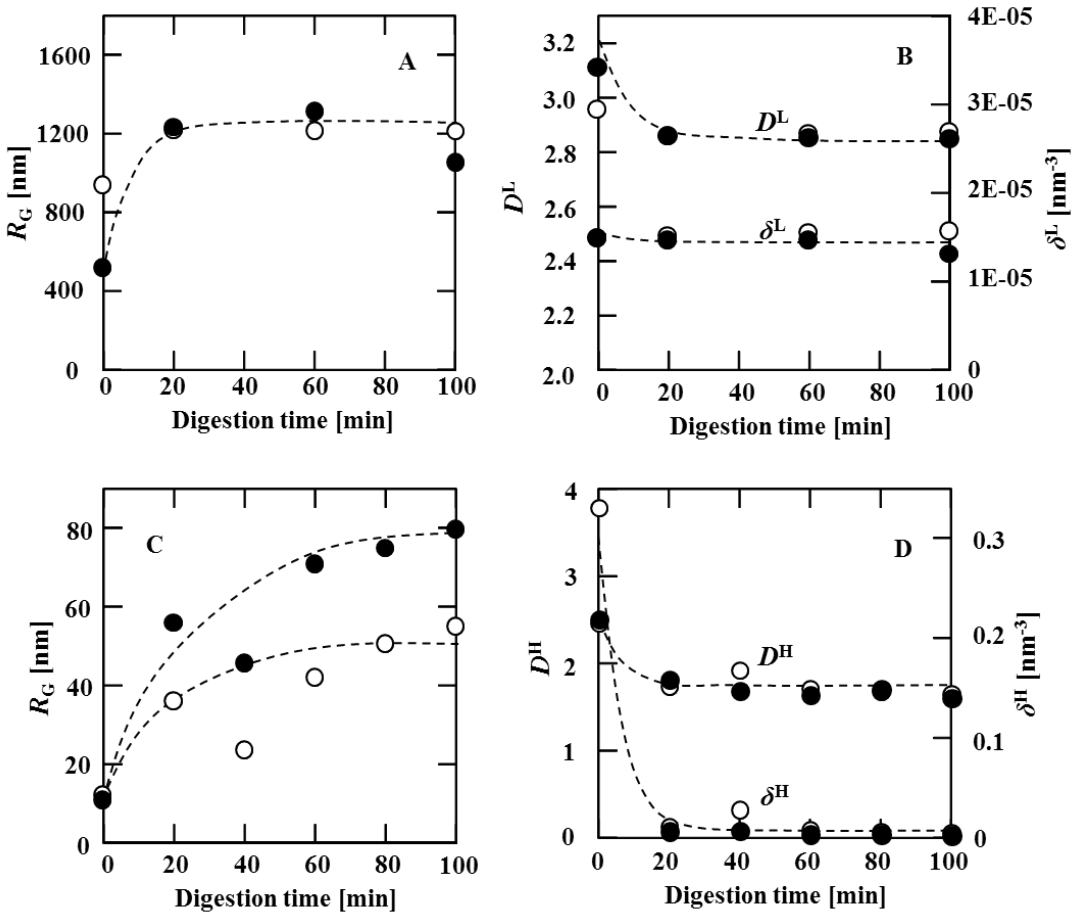

Figure 4–5: The structural parameters for A60-150 (○) and A60-180 (●): radius of gyration (R_G^L) obtained from the lower q region (A); fractal dimension (D^L) and density index (δ^L) obtained from the lower q region (B); radius of gyration (R_G^H) obtained from the higher q region (C); and the fractal dimension (D^H) and density index (δ^H) obtained from the higher q region (D). A60-150: casein clusters prepared with pH adjustment to 6.0, spray-dried at 150°C; A60-180: casein clusters prepared with pH adjustment to 6.0, spray-dried at 180°C.

4.4 Conclusions

Drying temperature and pH adjustment had a significant effect on the encapsulation efficiency and surface hydrophobicity of the obtained casein clusters. Adjusting the pH of the sodium caseinate solution to 6.0 improved the encapsulation efficiency, while the increased drying temperature resulted in decreased loading of β-carotene. On the other hand, pH adjustment and the increased drying temperature increased the surface hydrophobicity. The SAXS measurements suggested that the obtained casein clusters had a fractal structure with a rough surface, which was made up of many primary clusters. The cluster size of the pH-adjusted specimens was larger than the clusters obtained from the plain solution. The increased drying temperature resulted in an increase in the whole cluster size, whereas changes in the primary cluster, fractal dimension, and density index were not significant. The gastric digestion tests revealed that the digestion profiles for all the obtained casein clusters were similar, and about 30% of casein was digested within 120 min of digestion. All the obtained clusters grew with lower cluster density, while the rough, fractal-structured surface of the clusters was converted to a mass fractal structure under the digestion conditions. The influence of the drying temperature could obviously be seen through the change in the primary cluster size. The higher drying temperature gave larger primary clusters for the specimens prepared from the plain solution, whilst the clusters were smaller for the specimens obtained from the pH-adjusted solution.

Concluding Remark

This work aimed to investigate a new technique to prepare the casein cluster-based encapsulation system as a natural vehicle for encapsulation and controlled delivery of hydrophobic substances. The basic method used to prepare the dried casein cluster was simple that the sodium caseinate (SC) solution was mixed with hydrophobic substances, β-carotene, subsequently adjusting pH of the prepared solution followed by spray-drying.

For the preliminary study (chapter 2), we investigated the influence of pH values on the encapsulation efficiency (EE), size, and surface characteristic of the obtained casein cluster. The results suggested that the pH of the sodium caseinate solution, which determined the degree of aggregation, tremendously affected the encapsulation yield of β-carotene in the spray-dried powder. We found that at pH 6.0, the resultant powder showed excellent encapsulation property compared to other pH conditions (pH＝6.5, 5.5). The structural analyses showed that the pH condition also affected the physical properties of casein clusters that the cluster growth while the fractal dimension decreased with decreasing pH.

In the third chapter, we investigated the influence of cluster types (aggregated casein formed by adjusting the solution pH and re-assembled micelles prepared by the addition of salts) and aging on their properties. The representative of aggregated casein was selected from the results of the preliminary study that is the specimen prepared at pH 6.0, which was the highest value in EE. The EE of aggregated casein was higher than that of the re-assembled casein micelles. Aging the

solution of casein aggregated increased the encapsulation efficiency and simultaneously decreased the amount of free β-carotene. Dried powders obtained from the aged solution also showed good stability in terms of β-carotene retention and color changes under 11%RH and 75%RH over 21 d. Moreover, the stability of spray-dried powders was closely linked to the nanostructures of the original clusters.

In the final chapter, we studied on the digestibility of the dried-casein cluster prepared from SC solution, plain or pH-adjusted (pH=6.0), and spray-dried at different inlet air temperatures (150°C and 180°C). A higher spray-drying temperature resulted in lower EE and higher surface hydrophobicities. The effects of drying temperature and pH on the amount of digested casein were not significant. The cluster structures changed during digestion; specifically, the cluster size increased both in the overall diameter and on the primary structure scale. The fractal characteristics changed from surface to mass fractals, and simultaneously, the cluster density decreased. The drying temperature affected the cluster size during digestion, and the trends were different in the specimens obtained from the plain and pH-adjusted solutions.

Finally, we can conclude that the casein cluster obtained from this simple technique, pH adjustment and aging, could be used as wall materials to encapsulate hydrophobic substance with high efficiency. The product quality can be improved by properly selecting processing conditions that affected cluster formation and the resultant structures, that consequently determined the EE and storage stability. The results of digestion test suggested that the design of protein-based encapsulation

systems with desirable digestibility and bioavailability could be available based on the knowledge obtained in this study.

References

Agudelo, R. A., Gauthier, S. F., Pouliot, Y., Marin, J., & Savoie, L. (2004). Kinetics of peptide fraction release during *in vitro* digestion of casein. *Journal of the Science of Food and Agriculture, 84*(4), 325–332.

Alizadeh-Pasdar, N., & Li-Chan, E. C. Y. (2000). Comparison of protein surface hydrophobicity measured at various pH values using three different fluorescent probes. *Journal of Agriculture and Food Chemistry*, *48*, 328–334.

Anarjan, N., Mirhosseini, H., Baharin, B. S., & Tan, C. P. (2011). Effect of processing conditions on physicochemical properties of sodium caseinate-stabilized astaxanthin nanodispersions. *Food Science and Technology, 44*, 1658–1665.

Anema, S. G., Lowe, E. K., & Li, Y. (2004). Effect of pH on the viscosity of heated reconstituted skim milk. *International Dairy Journal, 14*(6), 541–548.

Ao, J., & Li, Bo. (2013). Stability and antioxidative activities of casein peptide fractions during simulated gastrointestinal digestion *in vitro*: Charge properties of peptides affect digestive stability. *Food Research International*, *52*, 334–341.

Augustin, M. A., Sanguansri, L., Rusli, J. K., Shen, Z., Cheng, L. J., Keogh, J., & Clifton, P. (2014). Digestion of microencapsulated oil powders: *in vitro* lipolysis and in vivo absorption from a food matrix. *Food and Function*, *5*, 2905–2912.

Bassett, D.C. (1981). *Principles of Polymer Morphology*. Cambridge, Cambridge University Press.

Beristain, C. I., Vazquez, A., Garcia, H. S., & Vernon-Carter, E. J. (1996). Encapsulation of orange peel oil by co-crystallization. *LWT-Food Science and Technology*, 29(7), 645–647.

Beristain, C. I., Azuara, E., & Vernon-Carter, E. J. (2002). Effect of water activity on the stability to oxidation of spray-dried encapsulated orange peel oil using mesquite gum (*Prosopis Juliflora*) as wall material. *Journal of Food Science, 67* (1), 206–211.

Black, K. A., Priftis, D., Perry, S. L., Yip, J., & Byun, W. Y. (2014). Protein encapsulation via polypeptide complex coacervation. *ACS Macro Letters, 3*, 1088–1091.

Bremer, L. G. B. (1989). Theoretical and experimental study of the fractal nature of the structure of casein gels. *Journal of the Chemical Society, 85* (10), 3359–3372.

Burgain, J., Gaiani, C., Cailliez-Grimal, C., Jeandel, C., & Scher, J. (2013). Encapsulation of *Lactobacillus rhamnosus* GG in microparticles: Influence of casein to whey protein ratio on bacterial survival during digestion. *Innovative Food Science and Emerging Technologies*, *19*, 233–242.

Chardot, V., Banon, S., Misiuwianiec, M., & Hardy, J. (2002). Growth kinetics and fractal dimensions of casein particles during acidification. *Journal of Dairy Science, 85*, 8–14.

Chegini, G. R., & Ghobadian, B. (2007). Spray dryer parameters for fruit juice drying. *World Journal of Agricultural Sciences, 3*(2), 230–236.

Chung, C., Sanguansri, L., & Augustin, M. A. (2010). Resistant starch modification: Effects on starch properties and functionality as co-encapsulant in sodium

caseinate-based fish oil microcapsules. *Journal of food science, 75*(9), E636–E642.

Dalgleish, D. G., & Corredig, M. (2012). The structure of the casein micelle of milk and its changes during processing. *Annual Review of Food Science and Technology, 3*, 449–467.

de Vos, P., Faas, M. M., Spasojevic, M., & Sikkema, S. (2010). Encapsulation for preservation of functionality and targeted delivery of bioactive food components. *International Dairy Journal, 20*, 292–302.

Desai, K. G. H., & Park, H. J. (2005). Recent developments in microencapsulation of food ingredients. Drying Technology, 23, 1361–1394.

Desobry, S. A., Netto, F. M., & Labuza, T. P. (1997). Comparison of spray-drying, drum-drying and freeze-drying for β-carotene encapsulation and preservation. *Journal of Food Science*, *62* (6), 1158–1162.

Dupont, D., Mandalari, G., Mollé, D., Jardin, J., Rolet-Répécaud, O., Duboz, G., Léonil, J., Mills, C. E. N., & Mackie, A. R. (2010). Food processing increases casein resistance to simulated infant digestion. *Molecular Nutrition and Food Research*, *54*, 1677–1689.

Dziuba, J., Babuchowski, A., Smoczynski, M., & Smietana, Z. (1999). Fractal analysis of caseinate structure. *International Dairy Journal, 9*, 287–292.

Elzoghby, A. O., Abo El-Fotoh, W. S., & Elgindy, N. A. (2011). Casein-based formulations as promising controlled release drug delivery systems. *Journal of Controlled Release*, *153*, 206–216.

Elzoghby, A. O., Samy, W. M., Elgindy. N. A. (2012). Protein-based nanocarriers as promising drug and gene delivery systems. *Journal of Controlled Release, 161*, 38–49.

Elzoghby, A. O., Samy, W. M., Elgindy. N. A. (2013a). Novel spray-dried genipin-crosslinked casein nanoparticles for prolonged release of alfuzosin hydrochloride. *Pharmaceutical Research, 30* (5), 512–522.

Elzoghby, A. O., Helmy, M. W., Samy, W. M., & Elgindy, N. A. (2013b). Spray-dried casein-based micelles as a vehicle for solubilization and controlled delivery of flutamide: Formulation, characterization, and in vivo pharmacokinetics. *European Journal of Pharmaceutics and Biopharmaceutics, 84*, 487–496.

Elzoghby, A. O., Helmy, M. W., Samy, W. M., & Elgindy, N. A. (2013c). Novel ionically crosslinked casein nanoparticles for flutamide delivery: formulation, characterization, and in vivo pharmacokinetics. International journal of nanomedicine, 8, 1721–1732.

Esmaili, M., Ghaffari, S. M., Moosavi-Movahedi, Z., Atri, M. S., Sharifizadeh, A., Farhadi, M., ... & Moosavi-Movahedi, A. A. (2011). Beta casein-micelle as a nano vehicle for solubility enhancement of curcumin; food industry application. *LWT-food science and technology, 44* (10), 2166-2172.

Euston, S. R., Ur-Rehman, S., & Costello, G. (2007). Denaturation and aggregation of *β*-lactoglobulin—a preliminary molecular dynamics study. *Food Hydrocolloids*, *21*, 1081–1091.

Eynard, L., Iametti, S., Relkin, P., & Bonomi, F. (1992). Surface hydrophobicity changes and heat-induced modifications of α-lactalbumin. *Journal of Agricultural and Food Chemistry*, *40*, 1731–1736.

Fares, K., Landy, P., Guilard, R., & Voilley, A. (1998). Physicochemical interactions between aroma compounds and milk proteins: Effect of water and protein modification. *Journal of Dairy Science, 81*, 82–91.

Farrell Jr, H. M., Qi, P. X., Wickham, E. D., & Unruh, J. J. (2002). Secondary structural studies of bovine caseins: Structure and temperature dependence of β-casein phosphopeptide (1–25) as analyzed by circular dichroism, FTIR spectroscopy, and analytical ultracentrifugation. *Journal of protein chemistry, 21*(5), 307–321.

Fiori, F., & Spinozzi, F. (2010). *Innovative Technological Materials: Structural Properties by Neutron Scattering, Synchrotron Radiation and Modeling.* New York, Springer Science & Business Media.

Flores, F. P., Singh, R. K., Kerr, W. L., Phillips, D. R., & Kong, F. (2015). *In vitro* release properties of encapsulated blueberry (*Vaccinium ashei*) extracts. *Food Chemistry*, *168*, 225–232.

Fox, P. F., & McSweeney, P. L. H. (2003). *Advanced Dairy Chemistry*. New York: Kluwer Academic/Plenum Publishers.

Fox, P. F., & Brodkorp, A. (2008). The casein micelle: Historical aspects, current concepts and significance. *International Dairy Journal*, *18*, 677– 684.

Freltoft, T., Kjems, J. K., & Sinha, S. K. (1986). Power-law correlations and finite-size effects in silica particle aggregates studied by small-angle neutron scattering. *Physical Review B*, *33* (1), 269–275.

Gharsallaoui, A., Roudaut, G., Chambin, O., Voilley, A., & Saurel, R. (2007). Applications of spray-drying in microencapsulation of food ingredients: An overview. *Food Research International, 40*, 1107–1121.

Gibbs, B. F., Kermasha, S., Alli, I., & Mulligan, C. N. (1999). Encapsulation in the food industry: A review. *International Journal of Food Sciences and Nutrition*, 50, 213–224.

Gonnet, M., Lethuaut, L., & Boury, F. (2010). New trends in encapsulation of liposoluble vitamins. *Journal of Controlled Release, 146*, 276–290.

Goula, A. M., & Adamopoulos, K. G. (2005). Stability of lycopene during spray drying of tomato pulp. *LWT-Food Science and Technology, 38*(5), 479–487.

Guichard, E. (2006). Flavour retention and release from protein solutions. *Biotechnology Advances, 24*, 226–229.

Guillaume, C., Jiménez, L., Cuq, J. L., & Marchesseau, S. (2004). An original pH-reversible treatment of milk to improve rennet gelation. *International dairy journal, 14*(4), 305–311.

Guri, A., Haratifar, S., & Corredig, M. (2014). Bioefficacy of tea catechins associated with milk caseins tested using different *in vitro* digestion models. *Food Digestion, 5*(1–3), 8–18.

HadjSadok, A., Pitkowski, A., Nicolai, T., Benyahia, L., & Moulai-Mostefa. (2008). Characterisation of sodium caseinate as a function of ionic strength, pH and temperature using static and dynamic light scattering. *Food Hydrocolloids, 22*, 1460–1466.

Hayakawa, S., & Nakai, S. (1985). Contribution of hydrophobicity, net charge and sulfhydryl groups to thermal properties of ovalbumin. *Canadian Institute of Food Science and Technology Journal*, *18* (4), 290–295.

Hogan, S. A., McNamee, B. F., O'Riordan, E. D., & O'Sullivan, M. (2001). Microencapsulating properties of sodium caseinate. *Journal of Agricultural and Food Chemistry, 49*(4), 1934–1938.

Inglingstad, R. A., Devold, T. G., Eriksen, E. K., Holm, H., Jacobsen, M., Liland, K. H., … Vegarud, G. E. (2010). Comparison of the digestion of caseins and whey proteins in equine, bovine, caprine and human milks by human gastrointestinal enzymes. *Dairy Science and Technology*, *90*, 549–563.

Ixtaina, V. Y., Julio, L. M., Wagner, J. R., Nolasco, S. M., & Tomás, M. C. (2015). Physicochemical characterization and stability of chia oil microencapsulated with sodium caseinate and lactose by spray-drying. *Powder Technology, 27*, 126–34.

Jafari, S. M., Assadpoor, E., Bhandari, B., & He, Y. (2008). Nano-particle encapsulation of fish oil by spray drying. *Food Research International, 41*(2), 172-183.

Jaubert, A., Durier, C., Kobilinsky, A., & Martin, P. (1999). Structural organization of the goat casein micelle: effect of the physico-chemical environment (pH, temperature, ionic strength) on its mineral and protein composition. *International dairy journal, 9*(3), 369–370.

Jyothi, N. V. N., Prasanna, P. M., Sakarkar, S. N., Prabha, K. S., Ramaiah, P. S., & Srawan, G. Y. (2010). Microencapsulation techniques, factors influencing encapsulation efficiency. *Journal of microencapsulation, 27*(3), 187-197.

Knoop, A. M., Knoop, E., & Wiechen, A. (1979). Sub-structure of synthetic casein micelles. *Journal of Dairy Research, 46*(02), 347–350.

Koch, M. H. J., Vachette, P., & Svergun, D. I. (2003). Small-angle scattering: A view on the properties, structures and structural changes of biological macromolecules in solution. *Quarterly Reviews of Biophysics, 36*(2), 147–227.

Krishnan, S., Bhosale, R., & Singhal, R. S. (2005). Microencapsulation of cardamom oleoresin: Evaluation of blends of gum arabic, maltodextrin and a modified starch as wall materials. *Carbohydrate Polymers, 61*, 95–102.

Krishnan, S., Kshirsagar, A. C., & Singhal, R. S. (2005). The use of gum arabic and modified starch in the microencapsulation of a food flavoring agent. *Carbohydrate Polymers, 62*, 309–315.

Landy, P., Druaux, C., & Voilley, A. (1995). Retention of aroma compounds by proteins in aqueous solution. *Food Chemistry, 54* (4), 387–392.

Lee, C. H., Singla, A., & Lee, Yugyung, L. (2001). Biomedical applications of collagen. *International Journal of Pharmaceutics*, *221*, 1–22.

Lee, E. J., Khan, S. A., Park, J. K., & Lim, K. (2012). Studies on the characteristics of drug-loaded gelatin nanoparticles prepared by nanoprecipitation. *Bioprocess and Biosystems Engineering, 35*, 297–307.

Li, J., Ye, A., Lee, S. J., & Singh, H. (2012). Influence of gastric digestive reaction on subsequent *in vitro* intestinal digestion of sodium caseinate-stabilized emulsions. *Food and Function*, *3*, 320–326.

Lim, H.K., Tan, C.P., Bakar, J. & Ng, S.P. (2012). Effects of different wall materials on the physicochemical properties and oxidative stability of spray-dried

microencapsulated red-fleshed pitaya (*Hylocereus polyrhizus*) seed oil. *Food and Bioprocess Technology, 5*, 1220–1227.

Liu, Z. Q., Zhou, J. H., Zeng, Y. L., & Ouyang, X. L. (2004). The enhancement and encapsulation of Agaricus bisporus flavor. *Journal of food engineering, 65*(3), 391-396.

Liu, L., Fishman, M. L., Hicks, K. B., & Kende, M. (2005). Interaction of various pectin formulations with porcine colonic tissues. *Biomaterials, 26*, 5907–5916.

Liu, Y., & Guo, R. (2008). pH-dependent structures and properties of casein micelles. *Biophysical Chemistry, 136*(2), 67–73.

Liu, W., Ye, A., Liu, W., Liu, C., Han, J., & Singh, H. (2015). Behaviour of liposomes loaded with bovine serum albumin during *in vitro* digestion. *Food Chemistry*, *175*, 16–24.

Livney, Y. D. (2010). Milk proteins as vehicles for bioactives. *Current Opinion in Colloid & Interface Science*, *15*, 73–83.

Mackie, A., & Maciezanka, A. (2010). Colloidal aspects of protein digestion. *Current Opinion in Colloid and Interface Science*, *15*, 102–108.

Mandalari, G., Adel-Patient, K., Barkholt, V., Baro, C., Bennett, L., Bublin, M., … Mills, E. N. C. (2009). *In vitro* digestibility of β -casein and β -lactoglobulin under simulated human gastric and duodenal conditions: A multi-laboratory evaluation. *Regulatory Toxicology and Pharmacology*, *55*, 372–381.

Marchin, S., Putaux, J., Pignon, F., & Léonil, J. (2007). Effects of the environmental factors on the casein micelle structure studied by cryo transmission electron

microscopy and small-angle x-ray scattering/ultrasmall-angle x-ray scattering. *The Journal of Chemical Physics*, *126*, 045101.

Martinez, M. J., Farías, M. E., & Pilosof, A. M. (2011). Casein glycomacropeptide pH-driven self-assembly and gelation upon heating. *Food Hydrocolloids, 25*(5), 860–867.

McClements, D. J., & Li, Y. (2010). Review of *in vitro* digestion models for rapid screening of emulsion-based systems. *Food and Function*, *1*, 32–59.

McMahon, D. J., & McManus, W. R. (1998). Rethinking casein micelle structure using electron microscopy. *Journal of Dairy Science*, *81*, 2985–2993.

McSweeney, S. L., Mulvihill, D. M., & O'Callaghan, D. M. (2004). The influence of pH on the heat-induced aggregation of model milk protein ingredient systems and model infant formula emulsions stabilized by milk protein ingredients. *Food Hydrocolloids, 18*(1), 109–125.

Menéndez-Aguirre, O., Stuetz, W., Grune, T., Kessler, A., Weiss, J., & Hinrichs, J. (2011). High pressure-assisted encapsulation of vitamin D_2 in reassembled casein micelles. *High Pressure Research*, *31*(1), 265–274.

Mertens, H. D. T., & Svergun, D. I. (2010). Structural characterization of proteins and complexes using small-angle X-ray solution scattering. *Journal of Structural Biology*, 172, 128–141.

Moitzi, C., Portnaya, I., Glatter, O., Ramon, O., & Danino, D. (2008). Effect of temperature on self-assembly of bovine β-casein above and below isoelectric pH. Structural analysis by cryogenic-transmission electron microscopy and small-angle X-ray scattering. *Langmuir*, *24*, 3020–3029.

Nakagawa, K., Jarunglumlert, T., & Adachi, S. (2014). Microencapsulation of β-carotene by self-aggregated caseinates. *Japan Journal of Food Engineering*, *15*, 51–57.

Nakai, S. (1983). Structure-function relationships of food proteins with an emphasis on the importance of protein hydrophobicity. *Journal of Agriculture and Food Chemistry*, *37*, 676–683.

Nedovic, V., Kalusevic, A., Manojlovic, V., Levic, S., & Bugarski, B. (2011). An overview of encapsulation technologies for food applications. *Procedia Food Science, 1*, 1806–1815.

Okuro, P. K., de Matos Junior, F. E., & Favara-Trindade, C. S. (2013). Technological challenges for spray chilling encapsulation of functional food ingredients. *Food Technology and Biotechnology, 51* (2), 171–182.

Pai, D. A., Vangala, V. R., Ng, J. W., Ng, W. K., & Tan, R. B. (2015). Resistant maltodextrin as a shell material for encapsulation of naringin: Production and physicochemical characterization. *Journal of Food Engineering, 161*, 68–74.

Pan, K., Zhong, Q., & Baek, S. J. (2013). Enhanced dispersibility and bioactivity of curcumin by encapsulation in casein nanocapsules. *Journal of agricultural and food chemistry, 61*(25), 6036–6043.

Pan, K., Luo, Y., Gan, Y., Baek, S. J., & Zhong, Q. (2014). pH-driven encapsulation of curcumin in self-assembled casein nanoparticles for enhanced dispersibility and bioactivity. *Soft matter, 10*(35), 6820–6830.

Pignon, F., Belina, G., Narayanan, T., Paubel, X., Magnin, A., & Gésan-Guiziou, G. (2004). Structure and rheological behavior of casein micelle suspensions

during ultrafiltration process. *Journal of Chemical Physics*, *121*(16), 8138–8146.

Qi, P. X., Wickham, E. D., & Farrell Jr, H. M. (2004). Thermal and alkaline denaturation of bovine β-casein. *The protein journal, 23*(6), 389–402.

Qi, W., Su, R. X., He, Z. M., Zhang, Y. B., & Jin, F. M. (2007). Pepsin-induced changes in the size and molecular weight distribution of bovine casein during enzymatic hydrolysis. *Journal of Dairy Science*, *90* (11), 5004–5011.

Qian, C., & McClements, D. J. (2011). Formation of nanoemulsions stabilized by model food-grade emulsifiers using high-pressure homogenization: Factors affecting particle size. *Food Hydrocolloids, 25*(5), 1000–1008.

Qian, C., Decker, E. A., Xiao, H. & McClements, D. J. (2012). Inhibition of β-carotene degradation in oil-in-water nanoemulsions: Influence of oil-soluble and water-soluble antioxidants. *Food Chemistry*, *135*, 1036–1043.

Quek, S. Y., Chok, N. K., & Swedlund, P. (2007). The physicochemical properties of spray-dried watermelon powders. *Chemical Engineering and Processing: Process Intensification, 46*(5), 386–392.

Risso, P. H., Borraccetti, D. M., Araujo, C., Hidalgo, M. E., & Gatti, C. A. (2008). Effect of temperature and pH on the aggregation and the surface hydrophobicity of bovine κ-casein. *Colloid and Polymer Science, 286*(12), 1369–1378.

Roccia, P., Martínez, M. L., Llabot, J. M., & Ribotta, P. D. (2014). Influence of spray-drying operating conditions on sunflower oil powder qualities. *Powder Technology, 254*, 307–313.

Ruis, H. G., Venema, P., & van der Linden, E. (2007). Relation between pH-induced stickiness and gelation behaviour of sodium caseinate aggregates as determined by light scattering and rheology. *Food Hydrocolloids, 21*(4), 545–554.

Sáiz-Abajo, M. J., González-Ferrero, C., Moreno-Ruiz, A., Romo-Hualde, A., & González-Navarro, C. J. (2013). Thermal protection of β-carotene in re-assembled casein micelles during different processing technologies applied in food industry. *Food chemistry, 138*(2), 1581–1587.

Sanchez, V., Baeza, R., Galmarini, M. V., Zamora, M. C., & Chirife, J. (2013). Freeze-drying encapsulation of red wine polyphenols in an amorphous matrix of maltodextrin. *Food Bioprocess Technology, 6*, 1350–1354.

Sauer, A., & Moraru, C. I. (2012). Heat stability of micellar casein concentrates as affected by temperature and pH. *Journal of dairy science, 95*(11), 6339–6350.

Sava, N., Van der Plancken, I., Claeys, W., & Hendrickx, M. (2005). The kinetics of heat-induced structural changes of *β*-lactoglobulin. *Journal of Dairy Science*, *88*, 1646–1653.

Semo, E., Kesselman, E., Danino, D., & Livney, Y. D. (2007). Casein micelle as a natural nano-capsular vehicle for nutraceuticals. *Food Hydrocolloids, 21*(5), 936–942.

Shaikh, J., Bhosale, R., & Singhal, R. (2006). Microencapsulation of black pepper oleoresin. *Food Chemistry, 94*, 105–110.

Shanmugam, V. P., Kapila, S., Sonfack, T. K., & Kapila, R. (2015). Antioxidative peptide derived from enzymatic digestion of buffalo casein. *International Dairy Journal, 42*, 1–5.

Shapira, A., Assaraf, Y. G., Epstein, D., & Livney, Y. D. (2010a). Beta-casein nanoparticles as an oral delivery system for chemotherapeutic drugs: impact of drug structure and properties on co-assembly. *Pharmaceutical research, 27*(10), 2175–2186.

Shapira, A., Assaraf, Y. G., & Livney, Y. D. (2010b). Beta-casein nanovehicles for oral delivery of chemotherapeutic drugs. Nanomedicine: *Nanotechnology, Biology and Medicine, 6*(1), 119–126.

Shapira, A., Davidson, I., Avni, N., Assaraf, Y. G., & Livney, Y. D. (2012). β-Casein nanoparticle-based oral drug delivery system for potential treatment of gastric carcinoma: Stability, target-activated release and cytotoxicity. *European Journal of Pharmaceutics and Biopharmaceutics*, *80*, 298–305.

Shimizu, M., Saito, M., & Yamauchi, K. (1985). Emulsifying and structural properties of *β*-lactoglobulin at different pHs. *Agricultural and Biological Chemistry*, *49* (1), 189–194.

Shu, B., Yu, W., Zhao, Y., & Liu, X. (2006). Study on microencapsulation of lycopene by spray-drying. *Journal of Food Engineering, 76*(4), 664–669.

Singh, H., & Ye, A. (2013). Structural and biochemical factors affecting the digestion of protein-stabilized emulsions. *Current Opinion in Colloid and Interface Science*, 18, 360–370.

Sorensen, C. M., Cai, J., & Lu, N. (1992). Test of static structure factors for describing light scattering from fractal soot aggregates. *Langmuir*, *8*, 2064–2019.

Takahashi, S. (1978). Sodium borohydride as a reducing agent for preparing ninhydrin reagent for amino acid analysis. *The Journal of Biochemistry*, *83*, 57–60.

Tuyen, C. K., Nguyen, M. H., & Roach, P. D. (2010). Effects of spray drying conditions on the physicochemical and antioxidant properties of the Gac (Momordica cochinchinensis) fruit aril powder. *Journal of Food Engineering, 98*(3), 385–392.

Tan, H. L., & McGrath, K. M. (2012). Na-caseinate/oil/water systems: Emulsion morphology diagrams. *Journal of Colloid and Interface Science, 381*, 48–58.

Tavares, G. M., Croguennec, T., Carvalho, A. F., & Bouhallab, S. (2014). Milk proteins as encapsulation devices and delivery vehicles: Applications and trends. *Trends in Food Science and Technology, 37*, 5–20.

Voutsinas, L. P., Cheung, E., & Nakai, S. (1983). Relationships of hydrophobicity to emulsifying properties of heat denatured proteins. *Journal of Food Science*, *48*, 26–32.

Wagner, L. A., & Warthesen, J. J. (1995). Stability of spray-dried encapsulated carrot carotenes. *Journal of Food Science, 60* (5), 1048–1053.

Walstra, P. (1999). Casein sub-micelles: do they exist? *International Dairy Journal*, *9*, 189–192.

Wandrey, C., Bartkowiak, A., & Harding, S. E. (2010) *Encapsulation Technologies for Active Food Ingredients and Food Processing* (pp. 31–100). New York: Springer.

Waugh, D. F., & Noble, Jr. R. W. (1965). Casein micelles. Formation and structure. II. *Journal of the American Chemical Society, 87* (10), 2246–2257.

Waugh, D. F., Creamer, L. K., Slattery, C. W., & Dresdner, G. W. (1970). Core Polymers of Casein Micelles. *Biochemistry, 9* (4), 786–795.

Yazdi, S. R., & Corredig, M. (2012). Heating of milk alters the binding of curcumin to casein micelles. A fluorescence spectroscopy study. *Food chemistry, 132*(3), 1143–1149.

Yüksel, Z., & Erdem, Y. K. (2005). The influence of main milk components on the hydrophobic interactions of milk protein system in the course of heat treatment. *Journal of food engineering, 67*(3), 301–308.

Zhang, F., & Ilavsky, J. (2010). Ultra-Small-Angle X-ray scattering of polymers. *Journal of Macromolecular Science, Part C: Polymer Reviews*, *50*, 59–90.

Zhang, S., & Vardhanabhuti, B. (2014). Intragastric gelation of whey protein–pectin alters the digestibility of whey protein during *in vitro* pepsin digestion. *Food and Function*, *5*, 102–110.

Zhang, Y., & Zhong, Q. (2013). Encapsulation of bixin in sodium caseinate to deliver the colorant in transparent dispersions. *Food Hydrocolloids, 33*(1), 1–9.

Zimet, P., Rosenberg, D., & Livney, Y. D. (2011). Re-assembled casein micelles and casein nanoparticles as nano-vehicles for ω-3 polyunsaturated fatty acids. *Food Hydrocolloids, 25*(5), 1270–1276.

Zuidam, N. J., & Shimoni, E. (2010). *Encapsulation Technologies for Active Food Ingredients and Food Processing* (pp. 3–29). New York: Springer.

Acknowledgements

This dissertation would not have been successful without the help, support and encouragement of numerous people. I take this opportunity to thank all those people who made this thesis possible and an unforgettable experience for me.

First of all, I would like to express my sincere gratitude to Professor Maeda Koji for his guidance, kind supports and warm encouragement. I am very much thankful to him for accepted me as a Ph.D. student.

I am greatly indebted to Professor Shuji Adachi for taking me as a student and member of this laboratory, Division of Food Science and Biotechnology of Graduate School of Agriculture of Kyoto University. He provided me valuable advices with direction that was not only mentoring but also gave me the constructive criticisms, technical supports, and extensive discussions on my research work.

I would like to express my deeply appreciations to my supervisor, Associate Professor Kyuya Nakagawa, who first suggested me to apply for Ph.D. course. He truly made a difference in my life that offered me this great opportunity. This work would not have been possible without his guidance, understanding, helpful suggestions, and his responsible supervision.

I am grateful to Assistant Professor Takashi Kobayashi for his kind supports. A very special thanks goes out to Rumiko Kamiya for her special cares that are meaningful to me. She provided me kind supports and encouragement not only like a colleague, but also became my great friend and sister.

I would like to thank all the members of the laboratory: Inthira Koomyart, Takenobu Ogawa, Daming Gao, Yuki Sha, Yayoi Miyagawa, Kazutaka Katsuki,

Souma Fukuzawa, Keisuke Shintani, Ango Tamura, Haruka Sawada, Shinri Tamiya, Matsuzawa Yumi, Angie Crotet, Tiezheng Ma, Masashi Yoshino, Takao Roppongi, Hironori Nagamizu, Boonnakhom Tangkhavanich, for their warm welcome, helpful support, many unforgettable experiences and memories, we shared.

I take this opportunity to sincerely acknowledge the Japanese Government for the Monbukagakusho scholarship for providing financial support my research.

In conclusion, I would like to give thanks to my family for their supports they provided me through my entire life. Without their love, cares, and encouragements, I would have never become the person that I am today.

List of publications

Jarunglumlert, T., & Nakagawa, K. (2013). Spray Drying of Casein Aggregates Loaded with β-Carotene: Influences of Acidic Conditions and Storage Time on Surface Structure and Encapsulation Efficiencies. *Drying Technology, 31*(13-14), 1459–1465.

Nakagawa, K., Jarunglumlert, T., & Adachi, S. (2014). Microencapsulation of β-carotene by self-aggregated caseinates. *Japan Journal of Food Engineering, 15*(2), 51–57.

Jarunglumlert, T., Nakagawa, K., & Adachi, S. (2015). Influence of aggregate structure of casein on the encapsulation efficiency of β-carotene entrapped via hydrophobic interaction. *Food Structure, 5*, 42–50.

Jarunglumlert, T., Nakagawa, K., & Adachi, S. (2015). Digestibility and structural parameters of spray-dried casein clusters under simulated gastric conditions. *Food Research International, 75,* 166–173.

Nakagawa, K., Jarunglumlert, T., & Adachi, S. Structural changes in casein aggregates under frozen conditions affect the entrapment of hydrophobic materials and the digestibility of aggregates. *In submission*.